UiT The Arctic University of Norway

Department of Electrical Engineering

Technical Challenges and Solutions of a three-phase bidirectional two stage Electric Vehicle charger

Name: Babur Zaman Khan Mughal

Candidate No. 14

Master's thesis in Electrical Engineering…ELE-3900 May 2022

Title: Technical Challenges and Solutions of a three-phase bidirectional two stage Electric Vehicle charger	**Date:** May 15,2022
Subject Name: M-EL-3900 Master's Thesis, 2022	**Classification:** Open
Faculty: Faculty of Engineering Science and Technology	**Subject Code:** ELE- 3900
Master Program: Electrical Engineering	
Supervisor: Chittaranjan Pradhan	
Key Words: Electric Vehicle (EV), Two step three phase bidirectional charger, Microgrid, Vehicle-to-Grid (V2G)	

Preface

As the world is revolutionizing and getting into the digital age with the help of Electronics and Artificial Intelligence, engineers and researchers are leading towards a far better technological and sustainable world, especially with the advancement in the electric vehicle systems and their integration with the microgrids. Thus, this thesis presents a step forward towards the solution of load management between EVs and Microgrids.

First of all, I thank Allah Almighty who gave me strength and knowledge to complete this thesis. The truth is, I could not have achieved this success without my mentor's guidance. But before that, I would like to thank my parents, who are always there to support me, unconditionally love me, and undoubtfully understand me. Along with them, I would like to thank my supervisor, Chittaranjan Pradhan who have helped me in every step where I needed guidance and have been there to support me in the challenges throughout this period. I thank all my guiders who put all the hard work and efforts into achieving the results.

Narvik, 15 May 2022

Babur Zaman Khan Mughal

Abstract

The sustainability of the power grid owing to the building strain of the ever-growing demand for electrical energy urges innovative and more practical solutions that enable active participation of end-users in stable and reliable management of power systems. One of the emerging projections of such a two-way exchange of electrical power between the grid and consumers is the developing field of bidirectional energy trade between power providers and electric vehicle owners. A bidirectional, three-phase, two-stage off-board electric vehicle EV charger design is proposed in this research. The first stage acts as alternating current AC to direct current DC converter during charging operation and behaves as three phase inverter and power factor corrector when energy exchange is from vehicle to grid. The second stage is a bidirectional DC-DC level converter linked to the first stage by a DC bus. The grid side filter is designed to enable the grid interfacing without any significant power quality problems. The proposed design, topology and the devised control infrastructure are tested through simulations on MATLAB/Simulink platform by interfacing the charger to a three-phase AC microgrid and the results approve the performance of the proposed charging topology.

Abbreviations

EV	Electric Vehicle
VPP	Virtual Power Plants
V2G	Vehicle to Grid
G2V	Grid to Vehicle
DC	Direct Current
AC	Alternating Current
DG	Distributed Generator
DS	Distribution System
SOC	State of Charge
VAR	Volt Ampere Reactive
PMU	Phasor Measurement Unit
EVSE	EV supply equipment
THD	Total Harmonic Distortion
PFC	Power Factor Correction
SPWM	Switching Pulse Width Modulation
SCADA	Supervisory Control and Data Acquisition
SOP	Soft Open Point
SVR	Static Voltage Regulator
VPP	Virtual Power Plant
ZVS	Zero Voltage Solution

Nomenclature

i_g	Single-phase grid current
V_s	Convertor side voltage
L_1	Convertor side inductor
L_2	Grid side inductor
ω_{sw}	Switching frequency
ω_{res}	Resonance frequency
f_{res}	Switching frequency
f_{sw}	Resonance frequency
V_L	Voltage across inductor
ωt	Phase angel
I_{abc}	three-phase non-filtered current outputs of the LCL filter
I_d	Current used for error calculation with respect to I_{dref}
I_q	Current used for error calculation with respect to I_{qref}
K_P	PI controller incorporates proportional
K_i	PI controller integral coefficients
I_{ref}	Reference current that indicates the behavior of the converter
V_{abc}	three-phase non-filtered voltage outputs of the LCL filter
I_{ch}	Battery charging current
I_{dis}	Battery discharging current

Table of Contents

List of Tables

List of Figures

1 Introduction

The growing global connectivity along with challenges like depleting conventional energy resources and environmental concerns is positively urging the researchers to innovate modern alternate energy economical and eco-friendly solutions.

1.1 Background and Motivations

One of the emerging technological innovations in this regard is the utilization of Electric Vehicle (EV) batteries as a storage and backup solution for improvement in various electrical energy utilization scenarios by actively participating in demand response by either selling back stored energy or throttling charging rate. The concept of a high-density EV battery as a source to inject electrical power into the grid has enabled multiple benefits for EV owners i.e., revenue generation, grid congestion management via valley filling and peak shaving, the inclusion of more and more renewable resources for energy production, a backup source in case of emergency or blackout, reliability enhancement of microgrids through participation in Virtual Power Plants (VPP) etc. However, apart from these numerous advantages, the only drawback is the potential stress resulting in a reduced life span of EV batteries due to increased charge/discharge cycles. Thus, Vehicle to Grid (V2G) implementation on the industrial level still faces a lot of technical difficulties leaving room for novel research and development.

By the end of 2015, the total number of electric vehicles on the roads reached one million. To motivate the concept of clean energy type of transportation they introduced multiple policies to facilitate them [1]. The alarming concern of global warming and greenhouse emissions is leading to various new and innovative solutions in multiple aspects of life to adopt a greener and ecofriendly lifestyle both on a countrywide and individual level. There is reported to be a significant 27% contribution of greenhouse emissions in the USA by the transportation sector only in the year 2020 [2]. Thus, there is an evident global trend of shifting toward more environment friendly options in every aspect e.g., in the transportation sector the replacement of conventional fossil fuel operated transportation, the adaptation of EVs can be a revolutionary step toward a cleaner environment. The benefit being the possibilities to fuel up the EV from renewable greener energy production sources apart from conventional fuel-powered sources. Hence, the energy storage infrastructure i.e., batteries and their chargers are being actively researched to improve their efficiency. There are some serious problems EVs are still facing like expensive batteries and their limited life cycles [3], incremental cost, power quality issues

regarding EV chargers, and inefficiency in the charging circuitry of EVs. Power quality-related issues can be addressed by using active filters [4], [5].

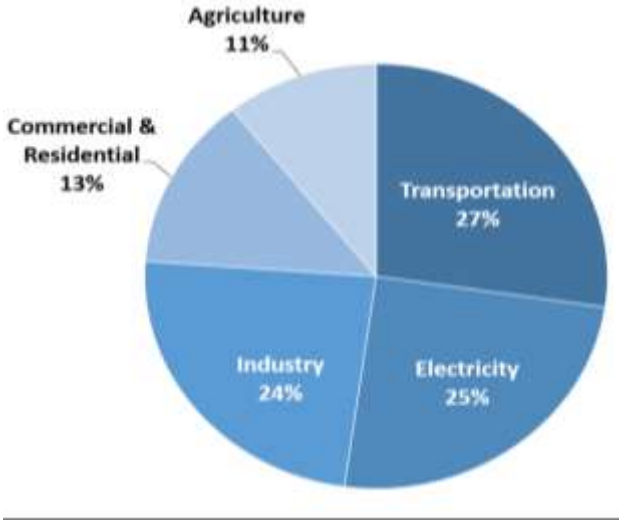

Figure 1: *Total Greenhouse Gas Emissions of USA by Economic Sector in 2020 [6].*

Usually, an on-board unidirectional charger is used with EVs that is a part of the vehicle itself and allows only the charging of EV battery via a flow of power from gird i.e., unidirectional Grid to Vehicle (G2V) operation. However, the relatively novel concept of V2G operation where an EV with stored energy can export its power back to the electrical grid ensures the numerous benefits stated above and it is very viable as the vehicle is parked for 85% of the time.

Based on the location of installation of EV battery charger, two classes have been specified in the literature.

- ***On-board Chargers*** are installed inside the electric vehicles operational on either single-phase or three-phase power sources. They being a part of EV add to its weight and volume that hinder the mobility somehow so, their power rating and size are limited [7], [8].
- ***Off-board chargers*** are fixed and installed at specific stations where an EV can get DC terminals of the battery attached for charging. As they do not affect the EV design so these types of chargers are usually high power rated and larger in size [9], [10].

V2G operation enables bidirectional power flows and allows the energy to be exchanged between vehicle and grid in either way. In specific V2G indicates the flow of active power from the vehicle to the grid, however, it can provide reactive power compensation also and the flow of reactive power is independent of the battery state of charge (SOC). The major advantage of reactive power support is that it can act like Var compensation and reduce losses of reactive power long-span transmission in grids by balancing the Var demand of load locally. On the other hand, charging from renewable sources during active hours and then feeding this energy during inactive hours can be an efficient solution to intermittent problems of renewable resources. The inherent limitation of power capacity of on-board chargers due to mobility of EV can be efficiently overcome by off-board chargers as they have high power ratings and are fixed so they can work under the agreement of ancillary services etc.

A vital aspect of V2G implementation is to enable communication between grid and vehicle for data exchange e.g., mode of operation, battery SOC etc. IEC 61850 [11] communication standard defines the standards to be followed for information exchange between intelligent electronic devices inside a substation while IEC 61850-7-420 [12] extension projects to the field of renewable energy generation infrastructure-related communication and IEC 61850-7-420 [13] extends to account for components that do not lie under the previous standards. However, the EVs and V2G operations were still unincorporated until 61850-90-8 [14] was proposed to fully accommodate EVs in smart grids. So accordingly, the EV utility grid can be connected to the EV via a so-called EV supply equipment (EVSE) and a charging outlet i.e., CHAdeMO, CCS/Combo, etc. The desirable characteristics of an EV charger are high efficiency, high power density, low power current ripple, bidirectional power flow and galvanic isolation etc. The high output current ripple negatively affects the battery lifespan.

1.2 Objectives

This research aims to design an off-board three-phase, 2 stages, and bidirectional EV charger suitable for both G2V and V2G mode by allowing bidirectional power exchange between vehicle and grid. The working and performance of the proposed design are to be tested through its integration with a three-phase AC microgrid composed of a combination of diesel generators with renewable energy sources i.e., wind and PV generation units. The operation of the proposed design scheme along with its control architecture is simulated using the MATLAB/Simulink platform to rigorously test the outcomes in both V2G and G2V modes.

1.3 Thesis Structure

This research proposes an off-board, 2 stages, bidirectional EV charger. The remainder of the thesis is organized as follows. **Chapter 2** elaborates on the related work and literature review on the topic. **Chapter 3** discusses the methodology of proposed work. **Chapter 4** focuses on modeling and simulations of the proposed topology of power electronic circuitry followed by **Chapter 5** significantly discusses the results and outcomes of simulations and comparison. Lastly, the performance of the proposed topology is summarized in the conclusion section in **Chapter 6**.

2 Literature Review

The petrol and diesel engines have some very negative impacts on the environment and human health. The emissions from petrol engines and diesel engines are very dangerous for the health of human beings, especially for children and the old ones. Those emissions can cause asthma, lung cancer, etc. in serious scenarios [15]. Furthermore, these emissions damage the lower-level ozone layer which protects vegetable crops and trees and these emissions are also the main cause of acidic rain which affects the drinking water and other essentials of a human being like vegetables, fish meat and animal meat etc. [16]. Due to all those non-eco-friendly features, the market growth of Electric Vehicles is increasing exponentially worldwide.

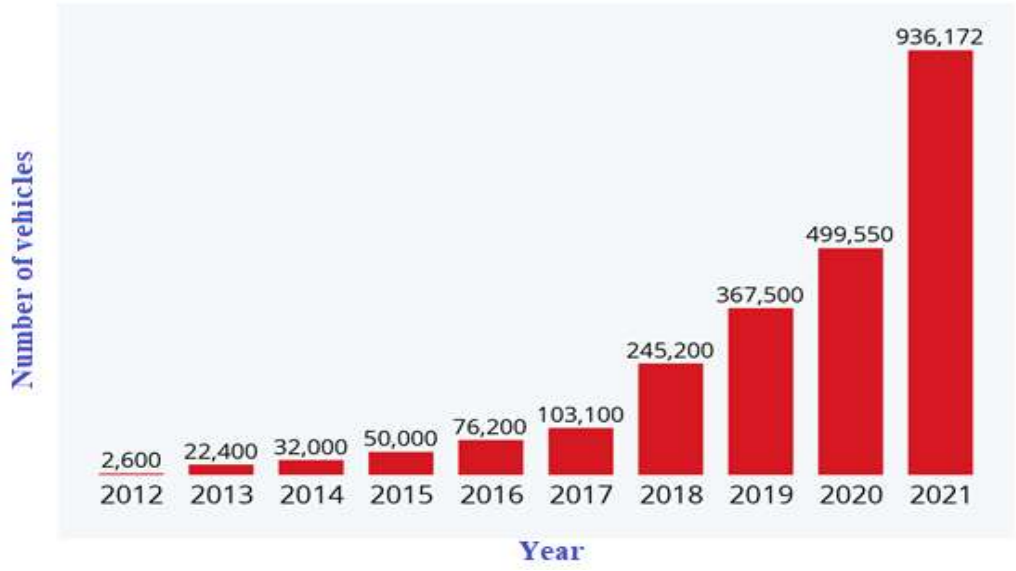

Figure 2: *Yearly sale of the Electric Vehicles units [14].*

However, with the increasing demand for EVs, some serious issue arises like the demand of electricity is increasing exponentially. In [17] suggested that the issue of the deficiency of electricity can be resolved by making photovoltaic generator-based EV charging stations. Those charging stations also have the capability of grid connection as during the absence of solar energy it can take energy from the grid to charge EVs.

San Diego Firm also worked on this adaptation and they designed the first solar-based standalone EV charging station However, the disadvantage of these strategies is that solar energy is mostly available from 8 AM to 5 PM during the daytime and this is the active timings for most of the jobs. To handle this problem [18] proposed to design renewable charging stations at workplaces where most people can charge their EVs during their job time. In [19] some methods are proposed to design a lightweight body of an EV to reduce the consumption of electricity. In [20] the issue of charging EVs is addressed by suggesting some methods of smart charging. Those methods are,

- Charging of EVs during off-peak hours.
- Charging EVs during the high availability of renewable energy sources links wind and solar.
- Charging EVs by remotely sensing the demand and supply patterns.

Smart charging can operate in two modes unidirectional charging and bidirectional charging. In unidirectional charging mode, EVs can be only charged like in G2V mode. In bidirectional charging mode, power can flow in both directions in V2G mode and G2V mode. A bidirectional charger has more advantages as it is capable to supply power back to the grid during peak hours. Charging of electric vehicles can be classified into two categories centralized [21], [22]or direct method and decentralized [23] or indirect method [24]. In the centralized or direct method, the EV charging is decided by an aggregator and in the indirect or decentralized approach, V2G or G2V mode is decided by the owner of the EV.

In [25] a multilevel AC-DC and DC-AC converter is used in bidirectional chargers as shown in **FIGURE 2**, with the integration of a buck/ boost converter. In G2V mode multilevel converter act as a rectifier and converts the AC voltage of the grid to DC voltage, a filter is used to make this DC voltage ripple-free. Then buck-boost converter acts as a buck converter and transforms high-level DC voltage to the battery level DC voltage. In V2G mode buck/boost converter acts as a boost converter and transforms battery level DC voltage to grid-level DC voltage and then through a multi-level converter that behaves like an inverter, this voltage is transformed to grid-level AC.

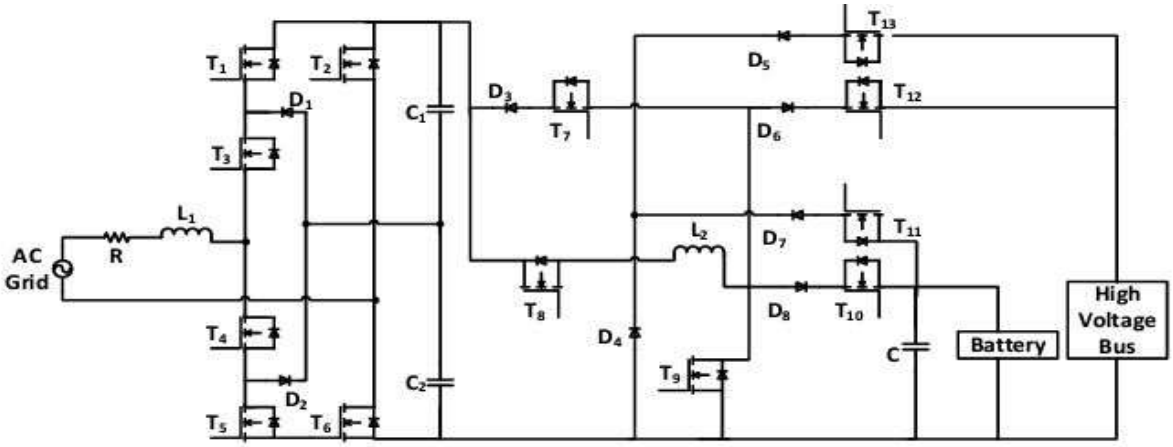

Figure 3: *Multilevel converter (AC-DC and DC-AC) interfaced with a buck/boost converter [26].*

In [26] a different topology of bidirectional charger is presented as shown in **FIGURE 3**. This model has the same functionality with the inclusion of a DC-DC converter and an AC-DC bidirectional converter. The control topology used in this formation is also responsible for sustaining the unity power factor and improving power quality. However, the issue of this topology is that it can achieve THD (Total Harmonic distortion) of just up to 8%. More number of switches are involved in this topology which is why more conduction loss occurs which is the main drawback of this topology.

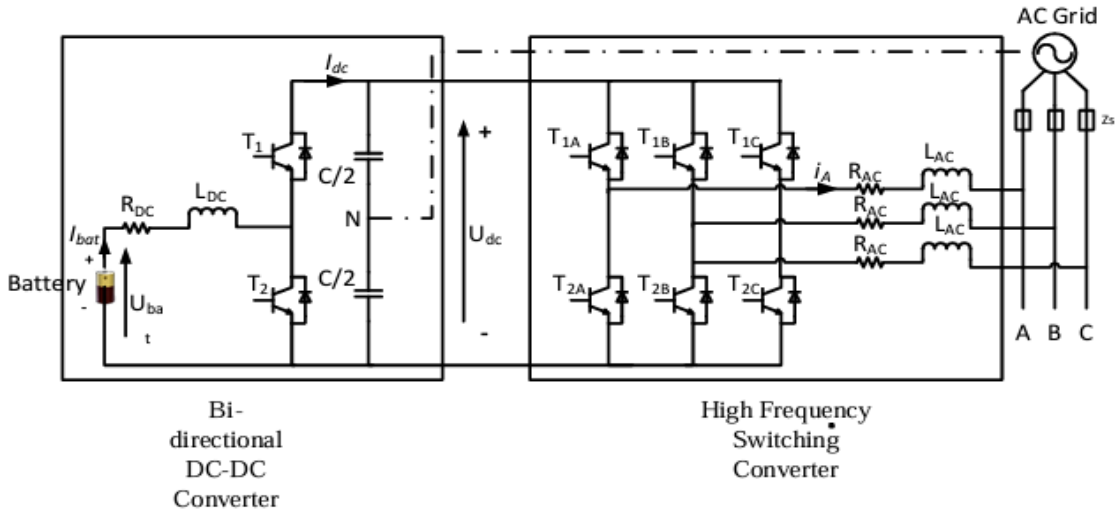

Figure 4: *Circuit diagram of a bidirectional charger with a bidirectional DC-DC Converter and a high-frequency switching converter [26].*

In [27] it is advised that to minimize the THD three-phase input is first transformed from AC-AC at higher frequency and battery level voltage through a step-down transformer. Then this voltage is transformed to DC through a rectifier as shown in **FIGURE 4**. Due to a greater number of switches, this topology again failed to impress due to the more conduction loss. This topology reduced the THD but low order harmonics remain the same.

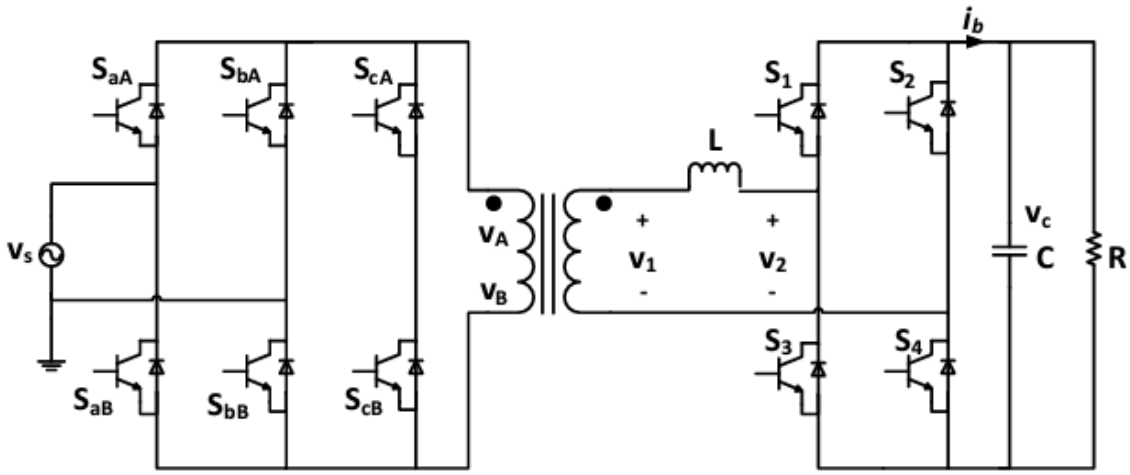

Figure 5: *Circuit of bi-directional charger explained in [27].*

In [28] another topology is introduced in which AC-AC conversion is done through a double active bridge [29] converter followed by a series resonant tank and a transformer to further step it down then through a single-stage converter, this AC voltage is rectified or inverted based on the direction of current or mode of operation as shown in **FIGURE 5**. The advantage of this topology is that more efficiency is achieved and soft switching phenomenon. However, again the disadvantage of this topology is the involvement of a greater number of switches and more conduction loss.

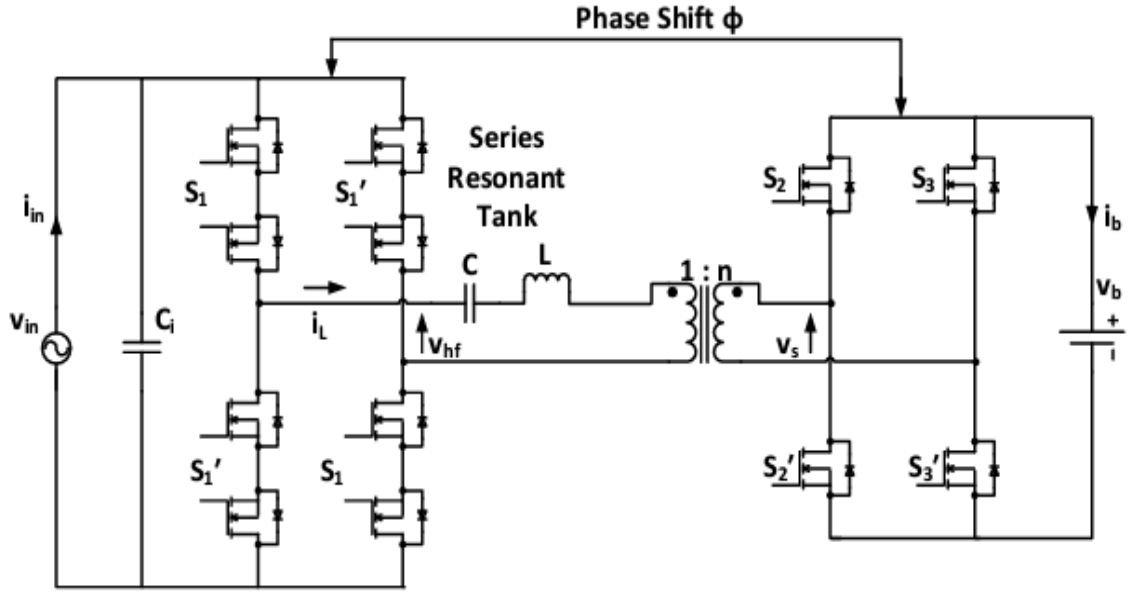

Figure 6: *Circuit diagram of a bidirectional charger presented in [29].*

In [30] a three-phase two-stage bidirectional charger for electric vehicles. The first stage was based on AC-DC and the second stage is for DC-DC conversion. Furthermore, the charger is modelled with a non-isolated converter based on a half bridge rectifier/inverter and the isolated converter based on a dual active bridge rectifier/inverter. The disadvantage of this charger is that it exchanges only active power so EV cannot be used as a static VAR compensator which is one of the benefits of EVs. The other disadvantage is that it takes a much longer time to stabilize or reach the steady state.

There are two classes of EV chargers based on the location of installation of a battery charger on-board charger [31] and off-board chargers [32]. On-board Chargers are installed inside the electric vehicles operational on either single-phase or three-phase power sources. They being a part of EV add to its weight and volume that hinder the mobility somehow so, their power rating and size are limited. Off-board chargers are fixed and installed at specific stations where an EV can get DC terminals of the battery attached for charging. As they do not affect the EV design so these types of chargers are usually high power rated and larger in size.

In specific V2G indicates the flow of active power from the vehicle to the grid, however, it can provide reactive power compensation also and the flow of reactive power is independent of the battery state of charge (SOC). The major advantage of reactive power support is that it can act like VAR compensation and reduce losses of reactive power long-span transmission in grids by balancing the Var demand of load locally. On the other hand, charging from renewable sources during active hours and then feeding this energy during inactive hours can be an efficient solution to intermittent problems of renewable resources. The inherent limitation of power capacity of on-board chargers due to mobility of EV can be efficiently overcome by off-board chargers as they have high power ratings and are fixed so they can work under the agreement of ancillary services etc. [33].

In this thesis, an off-board three phase, 2 stages, and bidirectional EV charger is designed for both G2V and V2G mode by allowing bidirectional power exchange between vehicle and grid. The working and performance of the proposed design is to be tested through its integration with a three-phase AC microgrid composed of the combination of a diesel generator with renewable energy sources i.e., wind and PV generation units. The operation of the proposed design scheme along with its control architecture is simulated using MATLAB/Simulink platform to rigorously test the outcomes in both V2G and G2V modes.

3 Modeling and Methodology of Proposed Work

A two-stage three phase, 100KVA bidirectional charger for high energy density EV batteries supporting both G2V (Charging) and V2G (Dis-charging) operations is designed. The major constitutes of the design topology are,

1. Designing of a Micro Grid
2. Grid Side LCL filter
3. three-phase Power Factor Correction (PFC) stage
4. Bidirectional voltage level converter stage

The design and control formulation along with parameter settings are elaborated in the following sections.

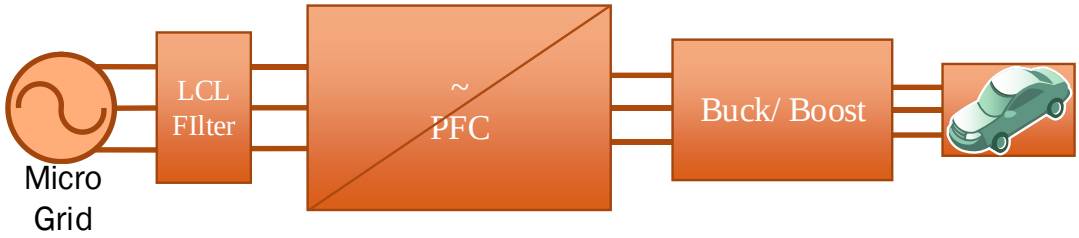

Figure 7: *The block diagram representing different stages of the designed bidirectional EV charger.*

During G2V mode, the vehicle takes energy from the microgrid and the battery charging process takes place where EV behaves as a conventional load to the microgrid. However, in V2G mode the EV can inject its stored energy into the microgrid as the battery discharges. The three-phase rectifier stage during charging mode behaves as a three-phase controlled grid-tied inverter/ power factor correction stage during V2G mode. The direction of current and power flow during both V2G and G2V modes are displayed in **FIGURE 8**.

3.1 Designing of a Micro Grid

A microgrid is a self-sufficient interconnected network of loads and distributed generation units that can work in two modes i.e., grid-connected and islanded. In grid-connected mode this network is connected with the main grid however in the islanded mode it is operating independently. The main difference between the main grid and a microgrid is the generation

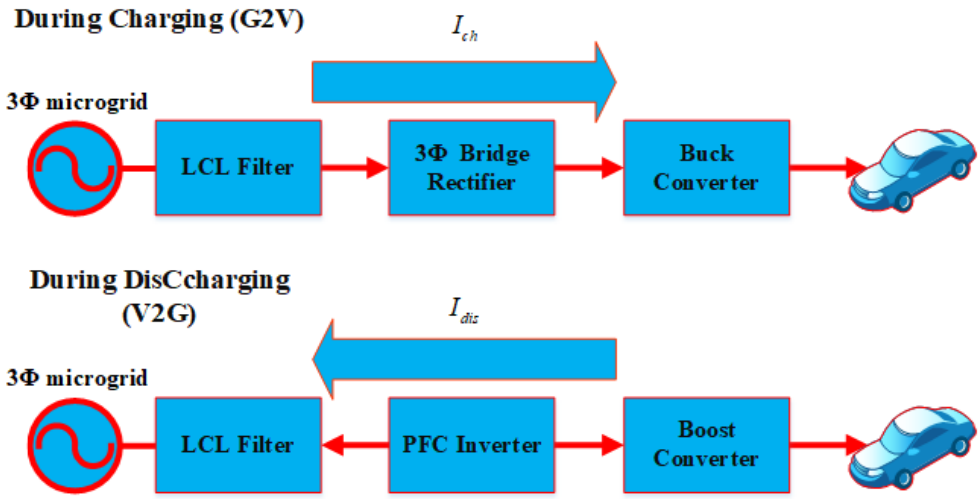

Figure 8: Power flow during V2G and G2V mode.

system and transmission line. Normally the main grid consists of a central generation system, and a large transmission network and can cover a large area. On the other hand, a microgrid contains distribution energy resources mainly consisting of wind distributed generators, photovoltaic distributed generators, and Electric Vehicles (EVs) in some cases. In this thesis, a bi-directional charger for Electrical Vehicles is designed that can work both in Grid to Vehicle (G2V) and Vehicle to Grid (V2G) during charging mode and discharging mode respectively.

A microgrid is designed by connecting multiple loads and multiple distributed generators on different nodes. To depict the real-time behaviors loads and generators are modelled stochastically.

3.2 Grid side LCL filter

LCL filter is used on the grid side to interface the EV charger with a three-phase grid. The major benefits of using LCL filters are reduction in switching frequency harmonics produced in the following stage of the circuit, reduce disturbance of sensitive loads, loss reduction and overall reduced Total Harmonics Distortion (THD). The LCL filter ensures the quality of power injected into the grid in V2G operational modes. LCL filter having a capacitor branch bypasses higher switching harmonics thus the size of the required inductor is reduced additionally better decoupling between the filter and grid impedance due to the LCL filter providing lower current ripples across grid current [34] [35].

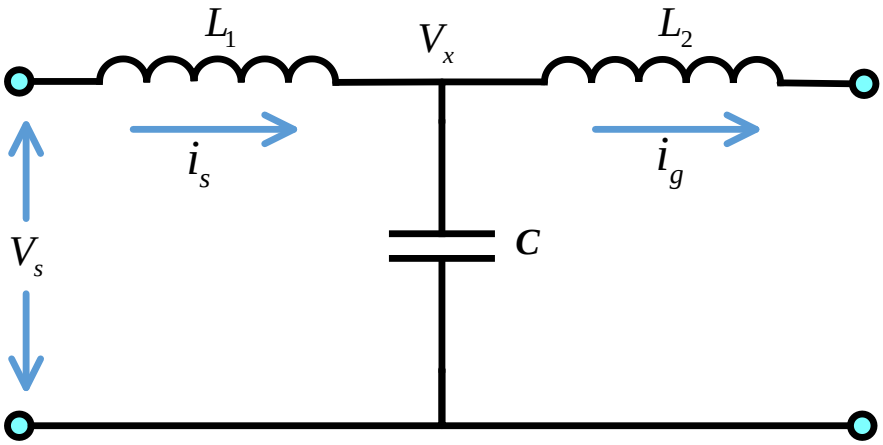

Figure 9: *Per-phase equivalent circuit of LCL filter.*

The per-phase equivalent circuit of the LCL filter is shown in **FIGURE 9**. Where, L_1 is convertor side inductor, L_2 is grid side inductor, i_g is single phase grid current and V_s is convertor side voltage. For simplicity the parasitic resistance of L_1, L_2, and C is considered to be ideally zero [36]. The transfer function of the given circuit is shown in Equation **(3.1)**

$$\frac{i_g}{V_s} = \frac{1}{j\omega L_2 + j\omega L_1 - j\omega^3 L_1 L_2 C} \tag{3.1}$$

3.2.1 Parameter Selection for Inductors

Manipulating the transfer function in Equation **(3.1)** to find the values of filter inductors gives us.

$$|L| = \left| \frac{1}{\omega_{sw}\left(\frac{i_g(sw)}{V_i(sw)}\right)\left(1-\frac{\omega_{sw}^2}{\omega_{res}^2}\right)} \right| \tag{3.2}$$

Where, $L = L_1 + L_2$, $i_g(sw)$ is the value of current at switching frequency, $V_i(sw)$ is the value of input voltage at switching frequency, ω_{sw} is the switching frequency and ω_{res} is the resonance frequency $\frac{1}{\sqrt{CL_f}}$, and

$$L_f = \frac{L_1 L_2}{L_1 + L_2}$$

Where, L_1 is the converter side inductor, and L_2 is the inverter side inductor [37]. According to IEEE standard, $i_g(sw) = 0.3\%$ of i_g, $V_i(sw) = 0.9\%$ of V_i, V_L is the voltage across inductor i.e. $V_L = 0.2 \times V_g$ for $L_{\max}$, where $\frac{L_{\max}}{2} = L_1 = L_2$. So, two equal valued inductors are applied in the LCL filter [38].

3.2.2 Parameter selection for Capacitor

The value of the capacitor is selected based on the well-known consideration that the reactive power requirement of the capacitor must be limited to 5% of the rated power of the power device. [39]

$$Q_c = 5\% \text{ of } S_{rated}$$

$$Q_c = \frac{V^2}{0.5\pi fC} = 5\% \text{ of } S_{rated}$$

$$C = \frac{(0.05)S_{rated}}{2\pi fV_g^2} \tag{3.3}$$

Where S_{rated} is the rated apparent power, Q_c is the reactive power of the capacitor, C is the value of the capacitor, V is the voltage and V_g is the single-phase voltage of the grid. As evident, the value of a capacitor depends upon frequency i.e., f_{res}, f_{sw} that ultimately depends upon device constraints, size, cost and thermal capabilities etc.

3.3 Three-phase Power Factor Correction Stage

The PFC stage consists of three phase bridge bidirectional rectifier/ inverter consisting of six power electronics switches controlled by voltage and current controls based on Park Clark transformation along with a phase-locked loop with feedback to ensure the unity power factor operation. Indirect control methods ensure improved performance parameters (both static and dynamic). The power electronics circuit of the three-phase power factor correction stage is shown in **FIGURE 10**.

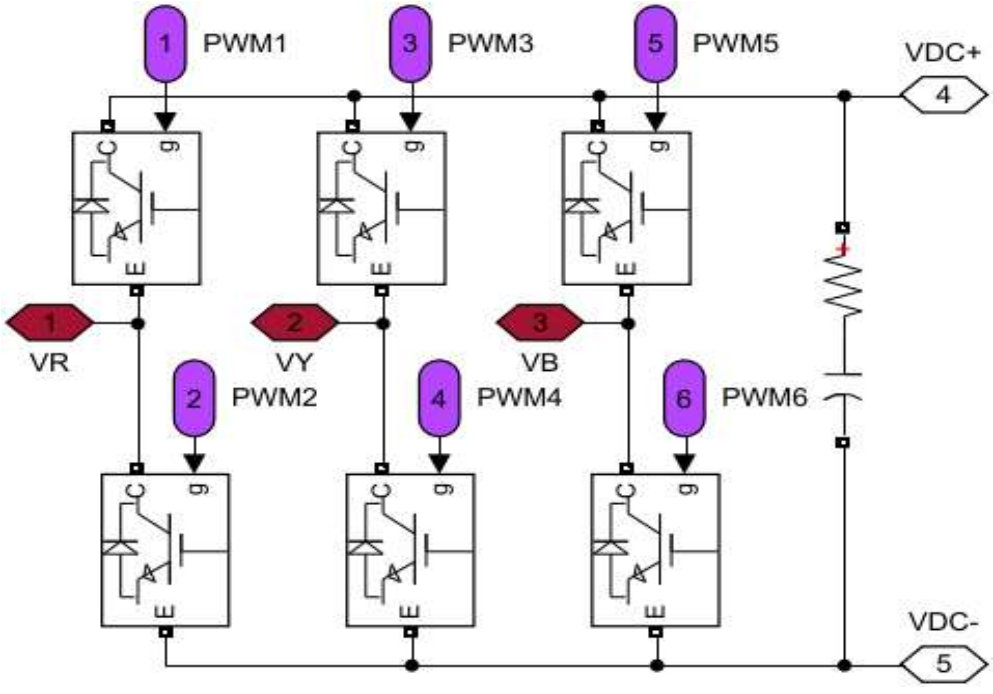

Figure 10: *Schematic Diagram of the three-phase power factor correction stage.*

The PWM control mechanism used for PFC stage switching control is explained below which maintains 800V constant DC at the DC bus of the PFC stage.

Let the three-phase voltage measured at the grid side be

$$V_g = [V_R \quad V_Y \quad V_B] \tag{3.4}$$

These voltages are transformed to $\alpha\beta 0$ and dq_0 domain respectively by applying the coordinate transformation. After applying $\alpha\beta 0$ transformation we get two-dimensional parameters where the third dimension is zero.

$$V_a = [V_\alpha \quad V_\beta] \tag{3.5}$$

These parameters are fed to the phase-locked loop controller as input. The controller generates phase angel (ωt) which is feedback to it also. The working of PLL is shown in **FIGURE 11**.

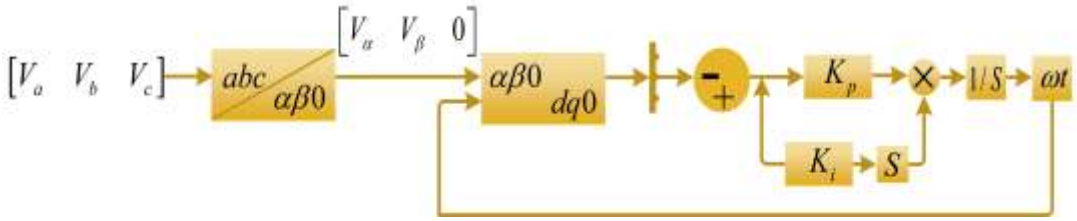

Figure 11: *Block diagram of phase lock loop working.*

Similarly, the three-phase non-filtered current outputs of the LCL filter I_{abc} are transformed to $\alpha\beta$ and then $dq0$ domain using (ωt) output of PLL. The resulting currents I_d and I_q are used for error calculation with respect to I_{dref} and I_{qref} which are in turn fed to PI. Current controllers. The resultant voltages after adding suitable gain to make it comparable to carrier wave amplitude are then transformed back to three-phase reference voltage parameters through inverse coordinate transformation. The reference voltage parameters are used as input for PWM generation that ultimately governs DC/AC conversion during V2G mode and vice versa.

The PWM generation uses a uni-polar SPWM scheme also known as 3 level modulation as shown in the block diagram below. The scheme reduces THD along with lower values of filtering inverter output and efficiency up to 98**%** due to reduced Zero Voltage Solution (ZVS) state losses [40].

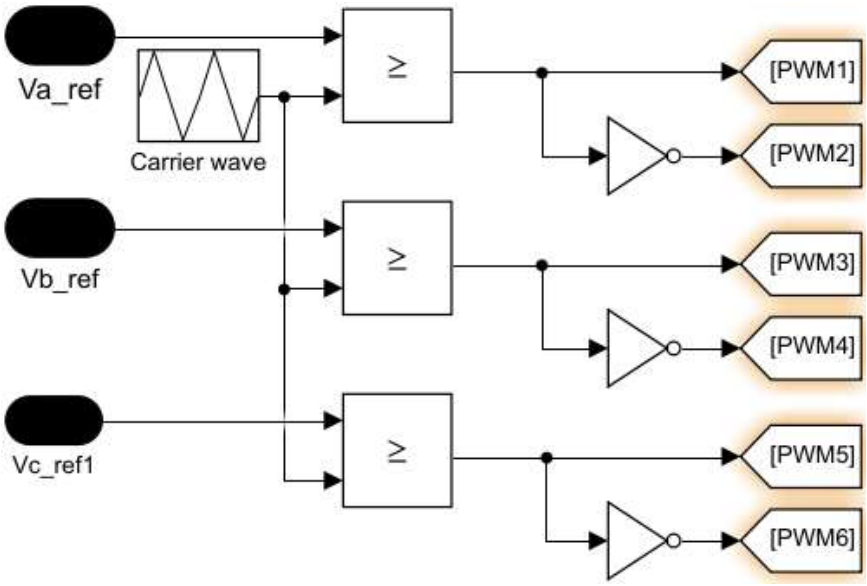

Figure 12: *Schematic diagram of sinusoidal PWM generation using unipolar modulation scheme.*

3.4 Bidirectional Voltage level converter stage

This stage consists of a bidirectional Buck/Boost converter. This stage works as a Buck converter when the charger is used in G2V mode operation and as a Boost converter. The current reference polarity decides the charging/discharging operation as it changes the direction of power flows PWM1 controls the upper switch performing buck operation while PWM2 controls the lower switch corresponding to boost operation.

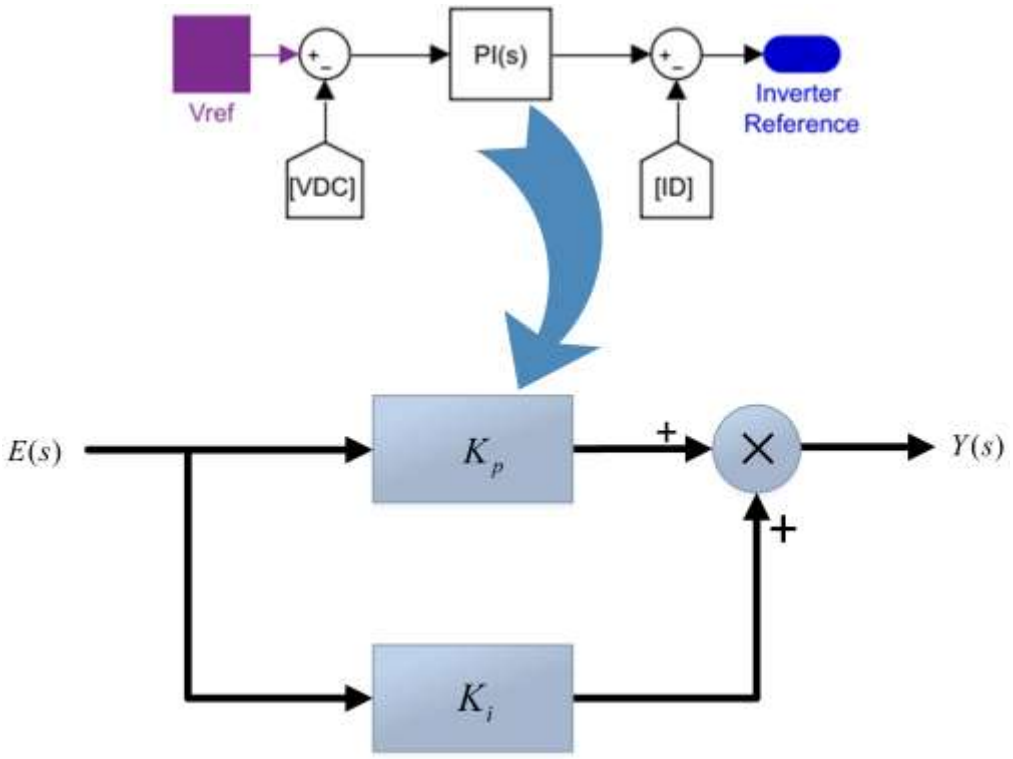

Figure 13: *Block diagram of PI internal function.*

The transfer function of the PI controller incorporates proportional and integral coefficients K_P and K_i resulting in the output relation given in Eq. **(3.6)**

$$Y(s) = E(s) \times \left(K_P + \frac{K_i}{S} \right) \tag{3.6}$$

The basic schematic of the three-phase grid-connected inverter s shown in **FIGURE 14**. DC voltage of a battery is taken as input and an inverter is designed by using BJTs and MOSFETS. The AC output of that inverter is then connected to the LCL filter which is explained already. Then the three-phase output of the LCL filter is connected to the grid. Then to design a controller three-phase voltage is transformed into two-phase V_α and V_β through parks transformation.

Then through these two voltages phase loop lock is implemented. Phase loop lock is already explained in detail in the previous section. Then V_α and V_β are transformed into E_d and E_q through Clark's transformation. On the other hand, all the three-phase currents are converted to I_α, I_β and then further converted to I_d and I_q by using parks and Clark's transformation.

Then these are transformed E_d, E_q, I_d and I_q are used for generating six PWMs for the BJTs/ MOSFETs of the inverter to synchronize the voltage, frequency, and shape of the sine wave to the microgrid.

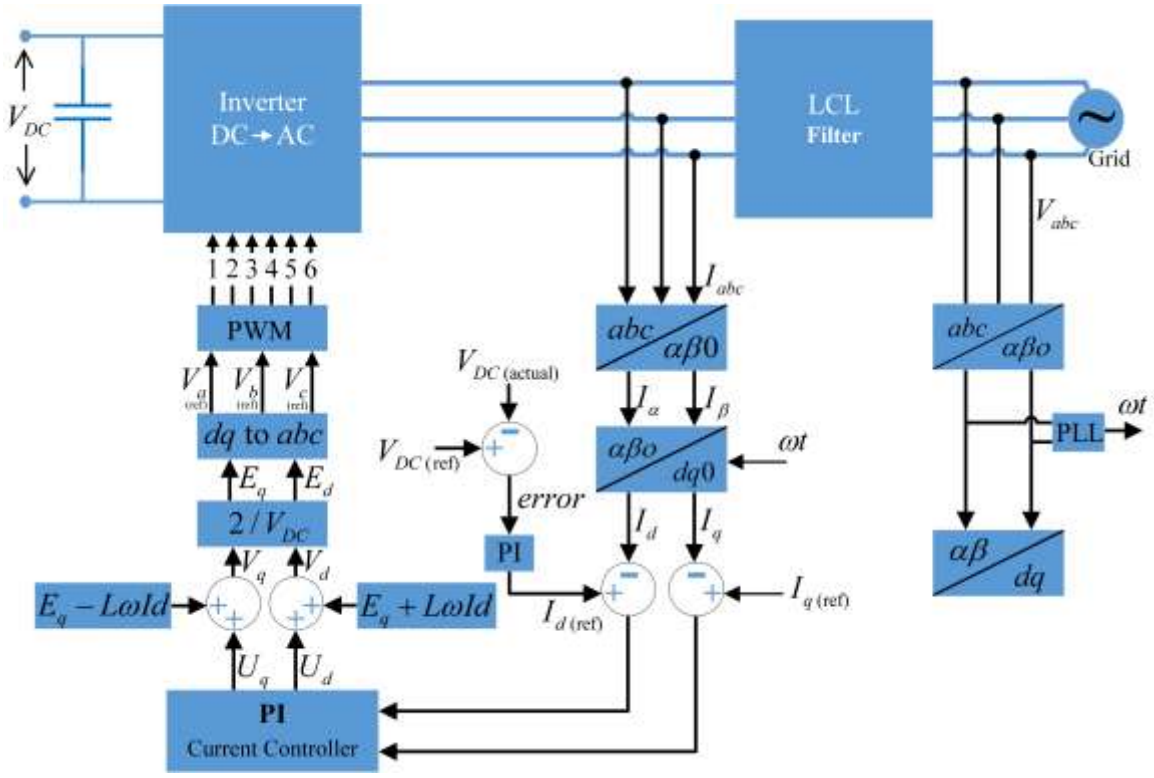

Figure 14: *Controller block diagram for three phase inverter PWM control to maintain VDC=800V at DC bus.*

I_{ref} is the current that indicates the behavior of the converter. Positive I_{ref} switch the converters behavior to charging mode or G2V mode, and Negative I_{ref} shows the converter is working in discharging and V2G mode as shown in FIGURE 15.

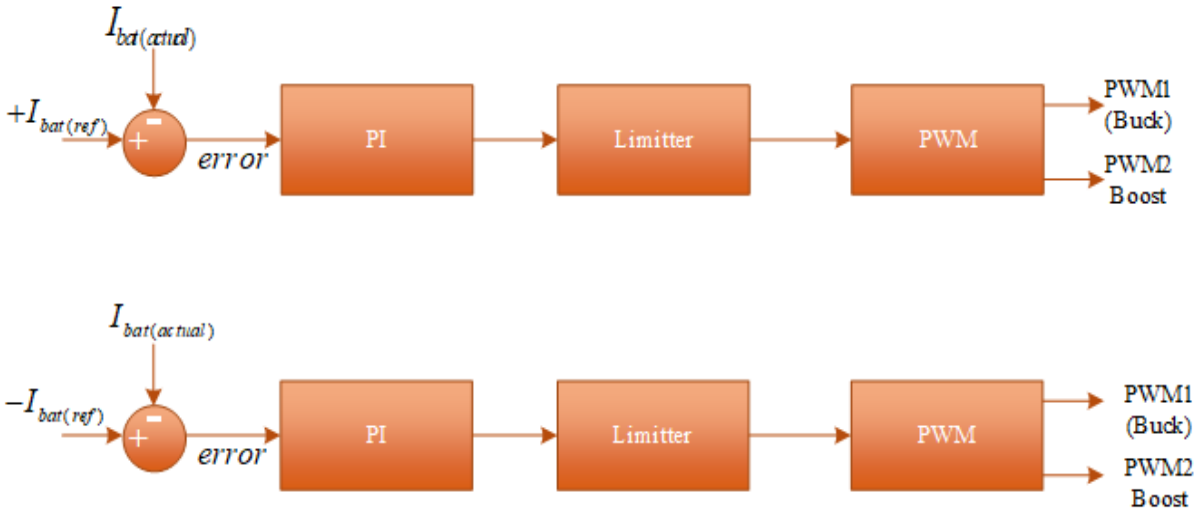

Figure 15: *For Battery charging and discharging.*

3.5 EV Battery Specifications:

The following TABLE 1 shows the battery specifications which have been chosen for this system.

Table 1: *Battery Specifications*

Parameter	Value
Nominal Voltage *(V)*	360*V*
Rated Capacity *(Ah)*	300*Ah*
Initial State of Charge *(%)*	50%
Battery Response Time *(s)*	1*s*
Battery Type	*Lithium-Ion*
Cut off Voltage *(V)*	270*V*
Fully Charged Voltage *(V)*	419.1*V*
Capacity at Nominal Voltage *(V)*	271.3*V*
Nominal Discharge Current *(A)*	130.43*A*
Internal Resistance *(Ohms)*	0.012 *Ohms*

4 Modeling and MATLAB Simulations of the Studied Power System with Results

This chapter describes the simulations and the results of the proposed bi-directional charger. The simulations are done on MATLAB R2020a. In the first step, a microgrid is designed that includes some distributed generators for islanded mode i.e., PV Generator, Wind Generator and a Diesel Generator and a main utility grid for the grid-connected mode. The main grid of 2500MVA / 132KV is used.

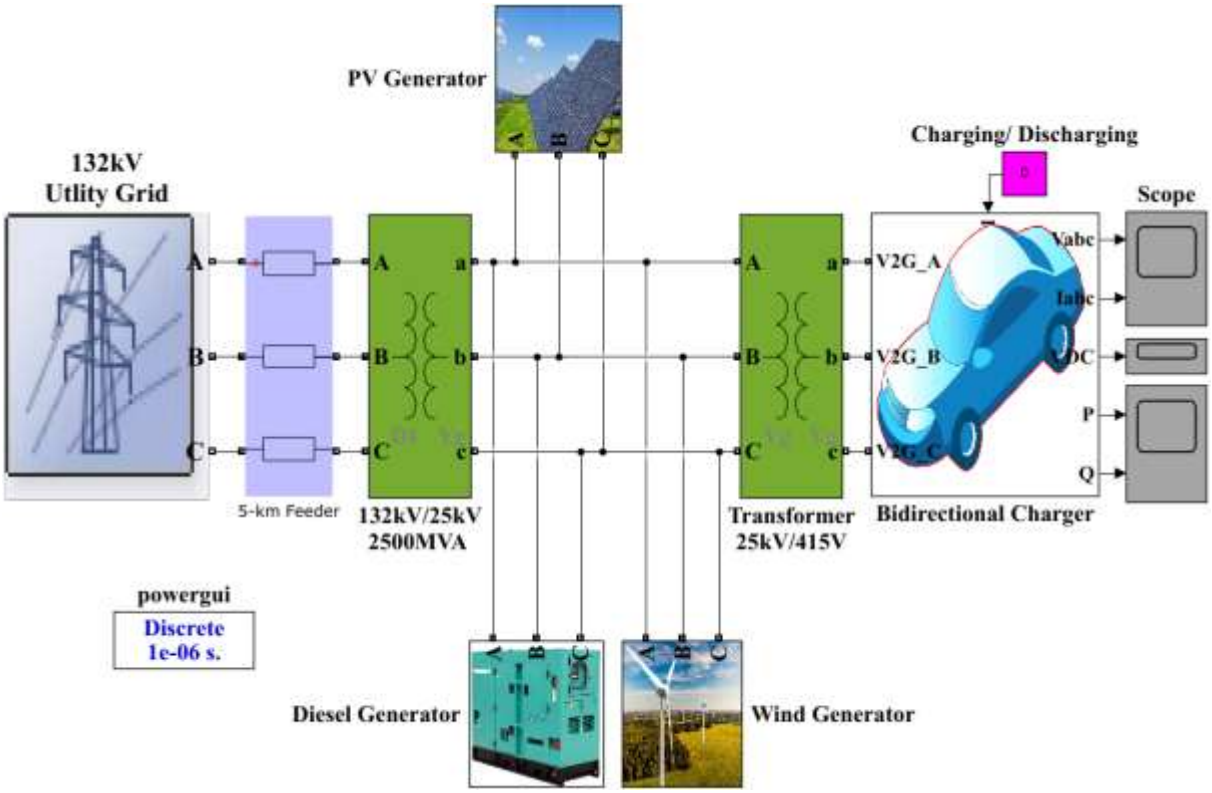

Figure 16: *The complete schematics of the proposed power system*

4.1 Microgrid

As the thesis is based on the designing of a bidirectional EV charger and its effects on the microgrid. So, for that purpose, a microgrid is designed that consists of main utility grid diesel generator, wind, generator, PV generator and bidirectional charger as shown in **FIGURE 16**.

4.1.1 Main Grid

A three-phase voltage source of 2500MVA/ 11KV is designed with a 50Hz frequency as shown in **FIGURE 17**. Then by using Star/Delta transformation a step-up transformer of 11KV/132KV is used before transmission to reduce the I^2R losses. A grounding transformer is used to protect the power network from fault. After that, a 14KM long transmission line is used to transfer the electricity from the main grid to the distribution grid.

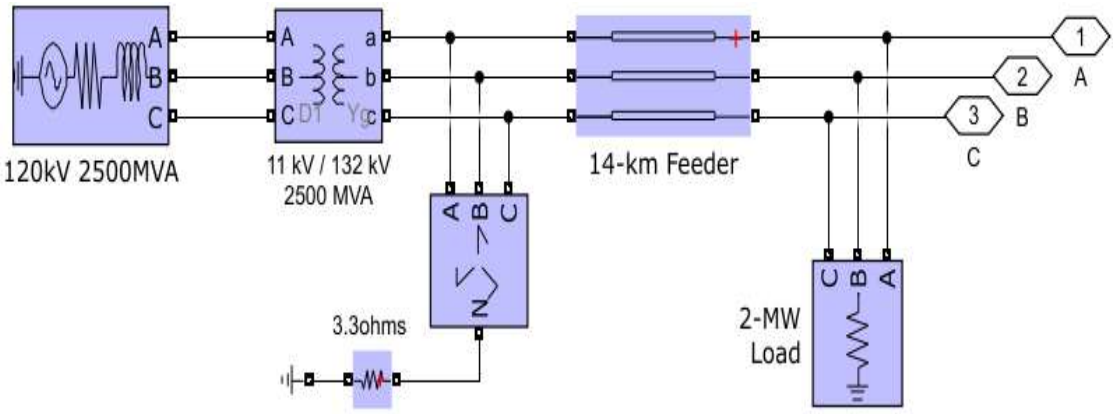

Figure 17: *2500MVA/ 120KV voltage source is modelled to operate as the main grid.*

4.1.2 PV Generator

A Photovoltaic Generator of 12KW is designed in Simulink MATLAB. A PV array of 66 solar panels is used that takes irradiance and temperature as input and generates DC power. By keeping the behavior of the solar energy, the dispatch curve is modelled for temperature and irradiance and given to the PV array module to depict the real-time behavior. All the parameters for the modelling of the PV array are shown in TABLE 2. Furthermore, a boost converter is used to step up the voltage to 500V DC. Then this DC Voltage is converted into three-phase AC voltage by using 3 level bridge inverter and further steps up to 25KV by using a three-phase delta/Star transformer as shown in FIGURE 18.

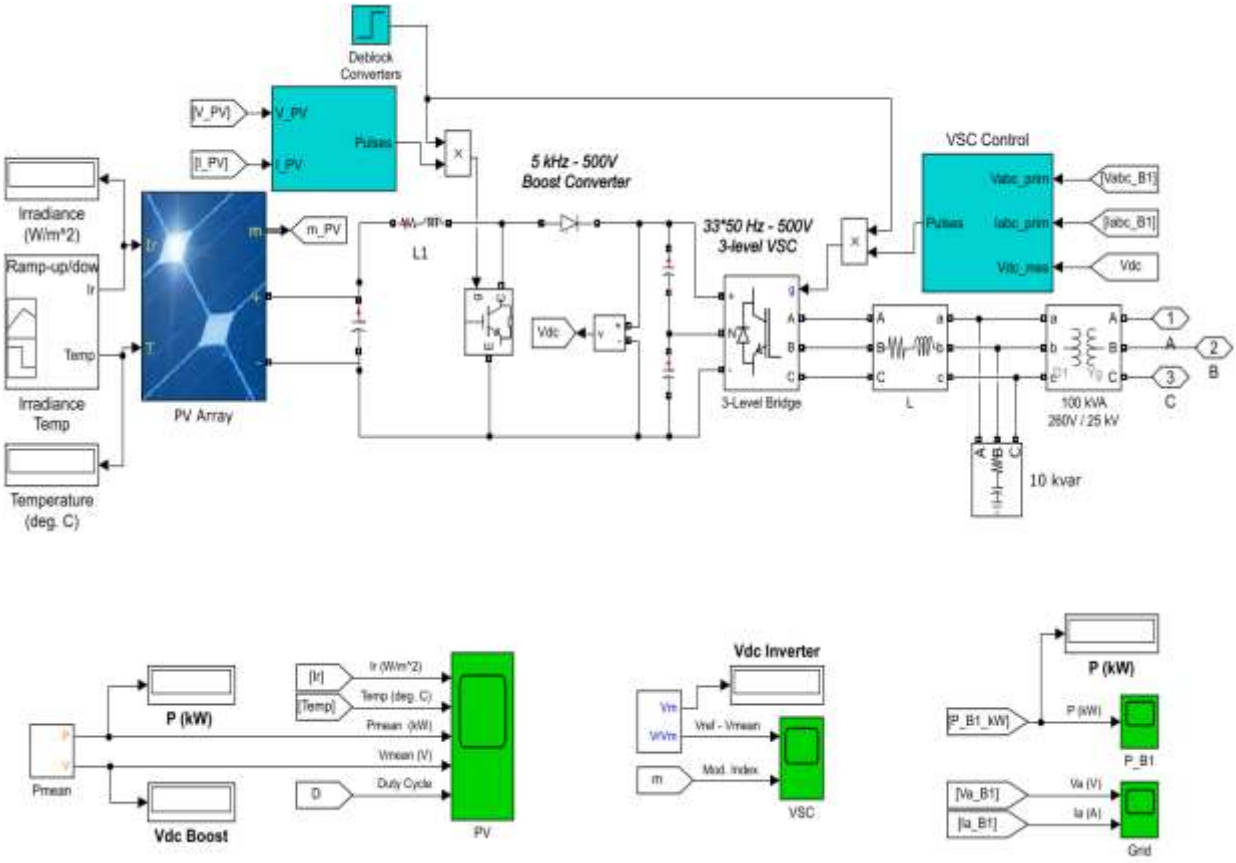

Figure 18: Simulink model of 12KW PV Generator.

Maximum power point tracking by incremental conductance method is used to obtain maximum power. Maximum power point is obtained when dP/*dV=0 where P= V*I.*

$$d(VI)/dV = I + VdI/dV = 0$$
$$dI/dV = -I/V \quad (3.7)$$

Where *dI* and *dV* are the fundamental components of I and V ripples measured with a sliding time window T_MPPT. *I* and *V* are the mean values of voltage and current measured with a sliding time window T_MPPT.

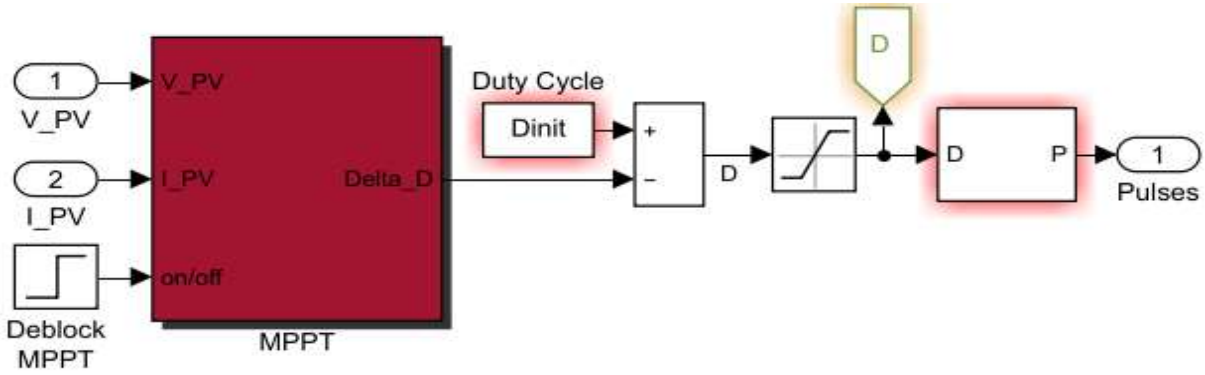

Figure 19: *The Simulink model of maximum power point tracking system for PV generator.*

The Simulink circuit of the VSC main control is shown in **FIGURE 20**. VSC Main Control is responsible for producing gate pulses for the three-phase inverter.

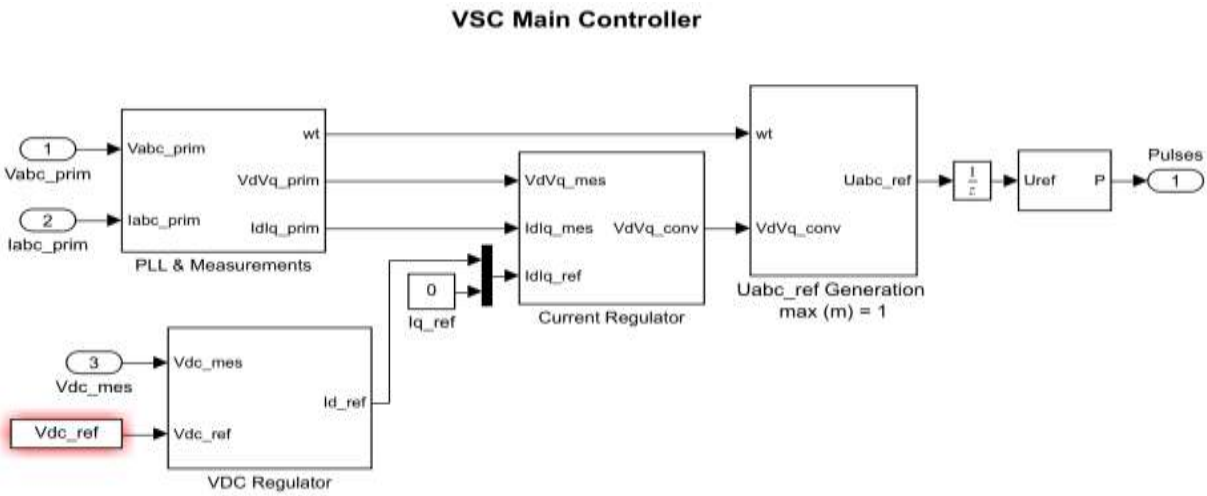

Figure 20: *Simulink Circuit of the VSC Main Controller that takes V_{abc} and I_{abc} and produces pulses for the three-phase inverter.*

Table 2: *Parameter for the PV modelling.*

Variable	Value
Parallel strings	66
Series connected module per string	5
Cells Per module (N_{cell})	96
Maximum Power per module	305.2W
Open Circuit Voltage (V_{oc})	64.2V
Voltage at maximum power point (V_{mp})	54.7V
Temp. Coefficent of V_{oc}	-0.27 *%/deg.C*
Short Circuit Current (I_{sc})	5.96A
Current at maximum power point (I_{mp})	5.58A
Temp. Coefficent of I_{sc}	0.062 *%/deg.C*
T_Cell	[0 25 50] *deg.C*
Series Resistance (R_s)	0.37152 *ohms*
Shunt Resistance (R_{sh})	269.59 *ohms*
Diode Ideality factor (D_0)	0.95

4.1.3 Wind Generator

A Wind Generator of 50KVA/400V is designed in MATLAB Simulink by keeping the wind behavior in mind. A block of wind induction turbine is used which takes two inputs wind and trip and provides three-phase AC as output. The trip is a binary input 1 is used to switch off the wind Generator and 0 is used to switch on the wind generator. The second input named wind is used to provide a dispatch curve to the wind generator. This block has built-in AC-AC conversion to have stable output. This three-phase AC is further stepped up to 25KV by using Delt/star transformation as shown in **FIGURE 21**. All the values of the parameters used in the modelling of wind generators are given in

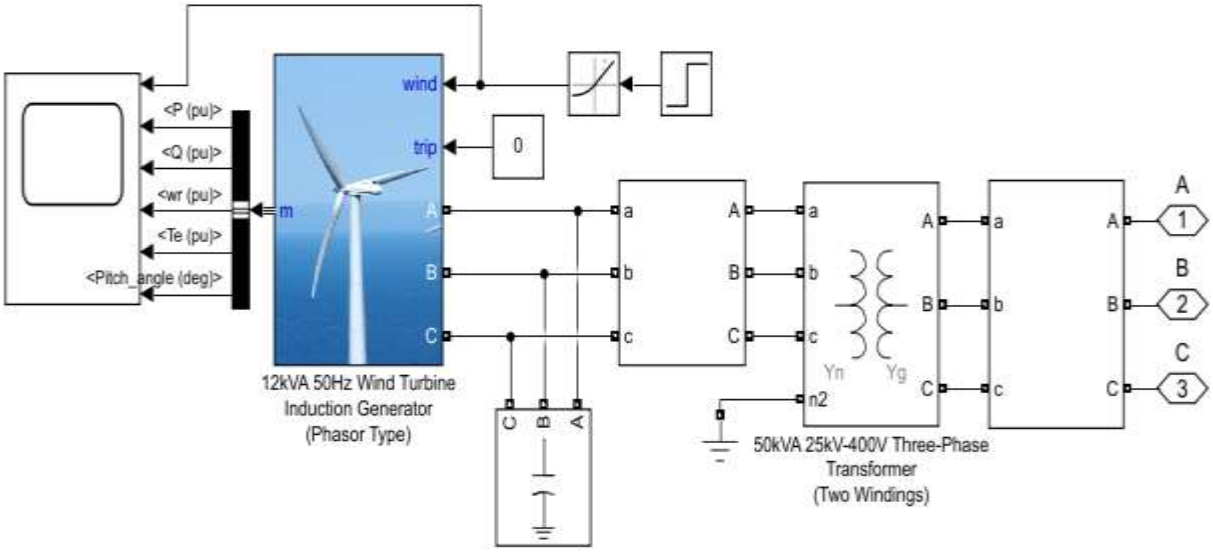

Figure 21: *Simulink model of 12KVA/ 400V wind generator.*

Table 3: *Parameter for the wind generator modelling.*

Variable	Value
Apparent Power (P_w)	50KW
Line voltage (V_n)	400V
Frequency (f)	50Hz
Stator Resistance (R_s)	0.004843 pu
Stator Inductance (L_s)	0.1248 pu
Rotor resistance (R_r)	0.004377 pu
Rotor Inductance (L_r)	0.1791 pu
Magnetizing inductance L_m (pu)	6.77 pu
Inertia constant	5.04 s
friction factor (F)	0.01 pu
pairs of poles (p)	3
Pitch angle beta	0 deg.
Nominal wind turbine mechanical output power	12 KW
Base wind speed	12 m/s
Base rotational speed	1 pu
Maximum power at base wind speed	1 pu
Proportional gain (K_p) of the PI-controller	2
Integral gain (K_i) of the PI-controller	25
Maximum pitch angle	45 deg.
The maximum rate of change of pitch angle	2 deg/s

4.1.4 Diesel Generator

A Diesel Generator of 15MVA/ 25KV is also used as a DG. A block of synchronous machines is used that takes two inputs. One is for connecting a prime mover for mechanical input and the other one is for excitation as shown in FIGURE 22. The diesel generator produces three-phase AC output that passed through an Isolation transformer of 1:1 that is used for safety purposes. Then these phase-to-phase voltages are measured by using voltmeters and displayed on the scope. Three ports of the three-phase AC are connected with the main grid in the main model. Some blocks are used to measure the electric power of the diesel generator and display it on the scope.

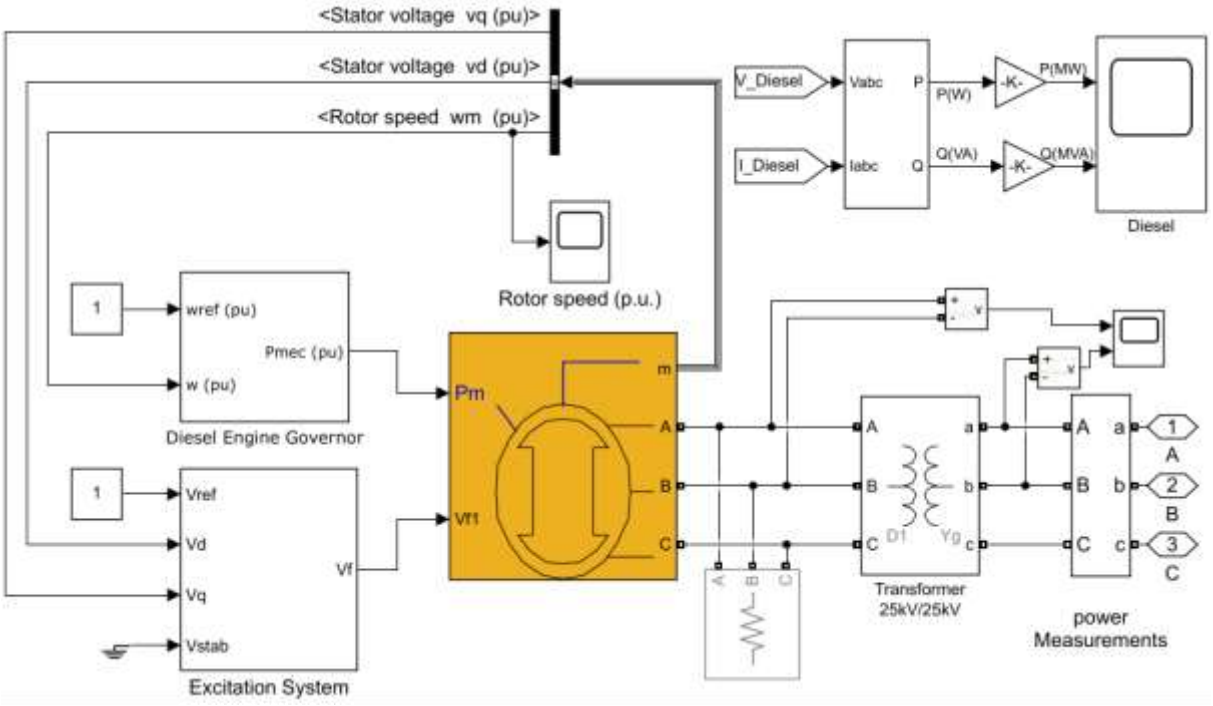

Figure 22: *Simulink model of 15MVA/ 25KV Diesel Generator.*

A prime mover/ Actuator system with a control scheme is implemented by keeping mechanical power in mind as shown in **FIGURE 23**. The built-in Simulink block of excitation system is used for V_{f1}.

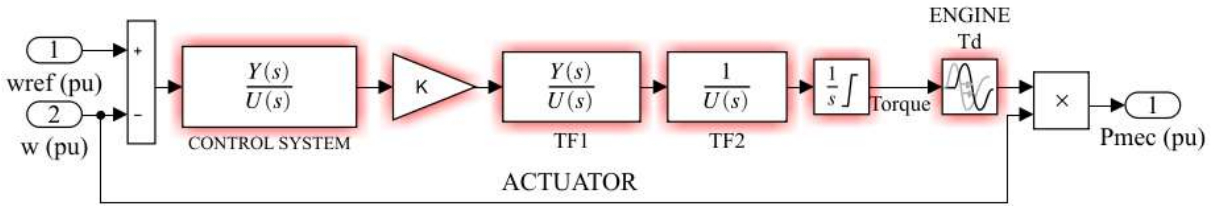

Figure 23: *Inside Simulink model of Diesel Engine Governor block.*

4.2 Bidirectional Charger

The main objective of this thesis is to design a three-phase bidirectional charger for an electric vehicle. The three phases of the input line from the mainline are connected to an LCL filter. A detailed description of an LCL filter is given in the previous section. The values of the inductor and capacitors are calculated by using **(3.2)** and **(3.3)**. Then the output of the LCL filter is passed through a three-phase controller. The three-phase controller can perform inverter operations or rectification operations based on the requirement as shown in **FIGURE 24**. Six PWMs are generated to control the switching of the IGBTs of the three-phase controller as shown in **FIGURE 14**. Then Buck or Boost operation is performed on DC voltage based on the charging operation (G2V) or discharging operation (V2G). While charging in G2V mode power is flowing from right to left fashion. Three-phase AC voltage is converted to DC through a three-phase rectifier and then to charge the battery DC voltage is stepped down by a buck converter at the voltage levels of the battery. While in V2G mode when the vehicle is transferring its power to the main grid, the DC voltage of the battery is stepped up by a boost converter and then transformed to a three-phase AC by using a three-phase inverter. Furthermore, this three-phase AC voltage is passed through an LCL filter and then connected with the grid. Current and voltages are transformed using Clarks and parks transformation and a phase loop lock is used to lock it with the grid. All the details regarding the transformations and phase loop lock are explained in the previous section. The Simulink models of the complete simulations are shown in **FIGURE 24**.

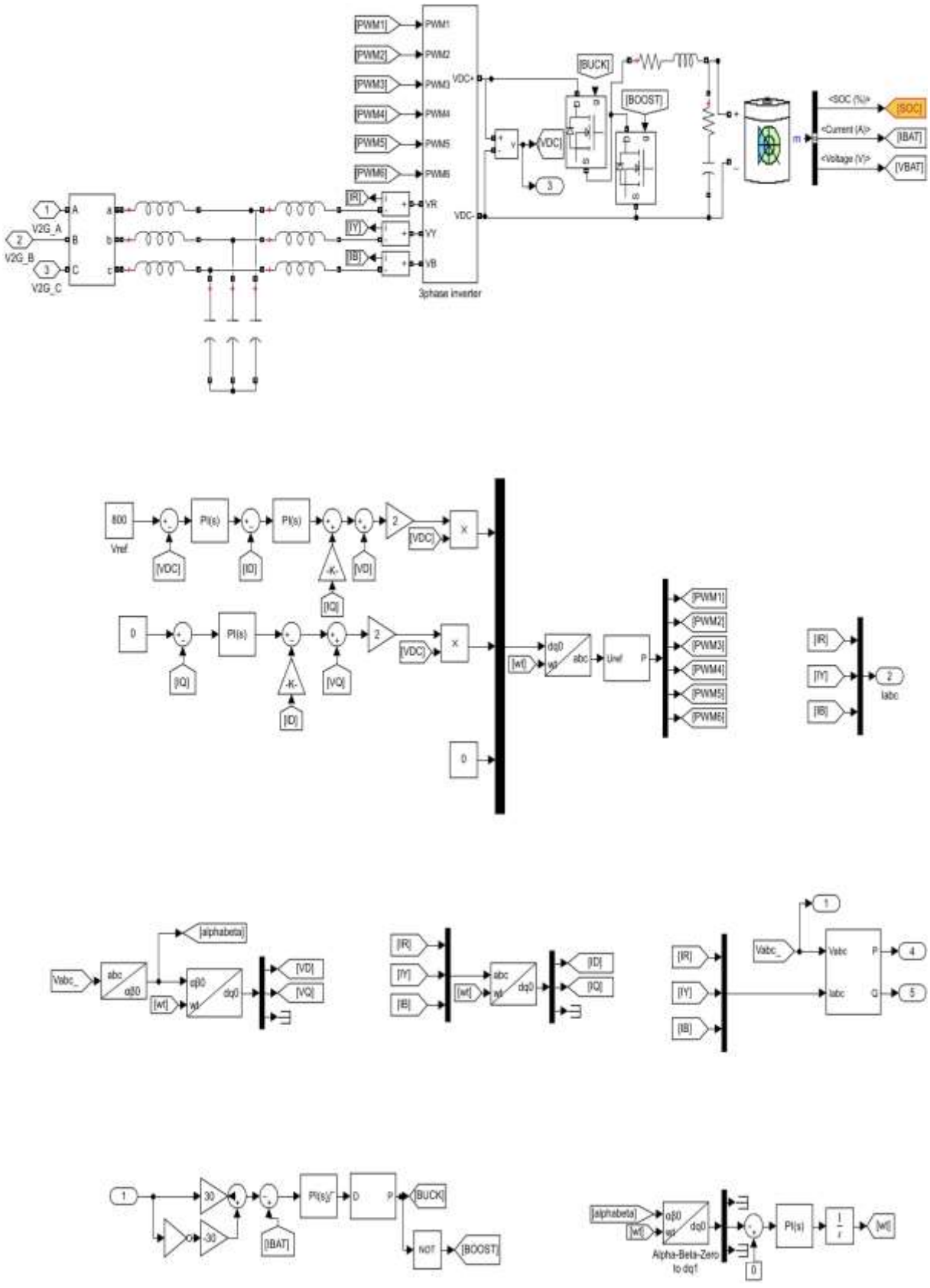

Figure 24: *The complete Simulink model of the bidirectional charger.*

The three-phase voltage from the main bus of all the synchronized generation units i.e., Utility grid, Diesel generator, Wind generator, and PV generator is displayed in FIGURE 25. The results display that all the phases of voltages are balanced 120 degrees apart.

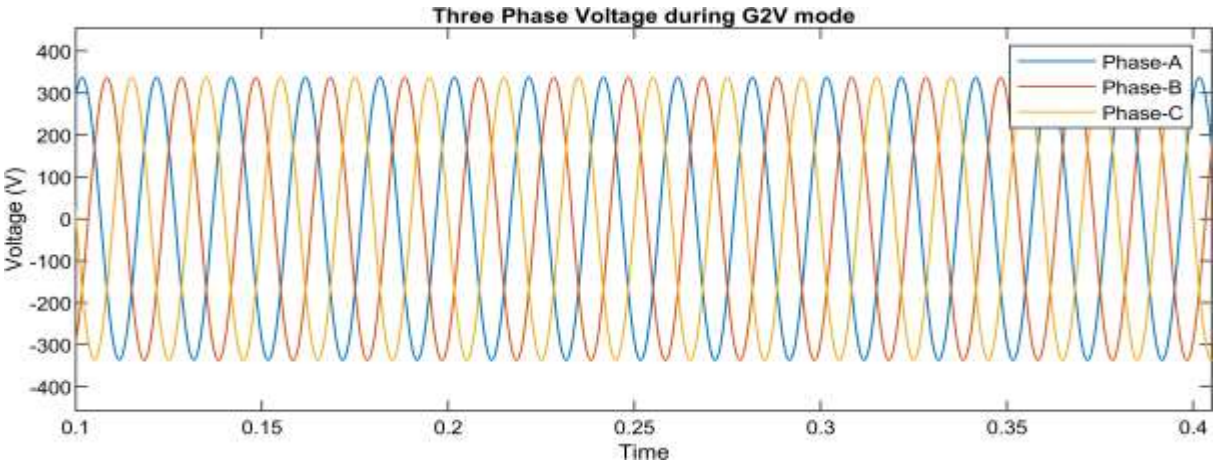

Figure 25: *In the above figure the graphs of three-phase voltages are shown for the charging mode.*

The three-phase current from the main bus of all the synchronized generation units i.e., Utility grid, Diesel generator, Wind generator, and PV generator are displayed in FIGURE 26. It indicates that all the phases are balanced, currents are in-phase and exactly 120 degrees apart.

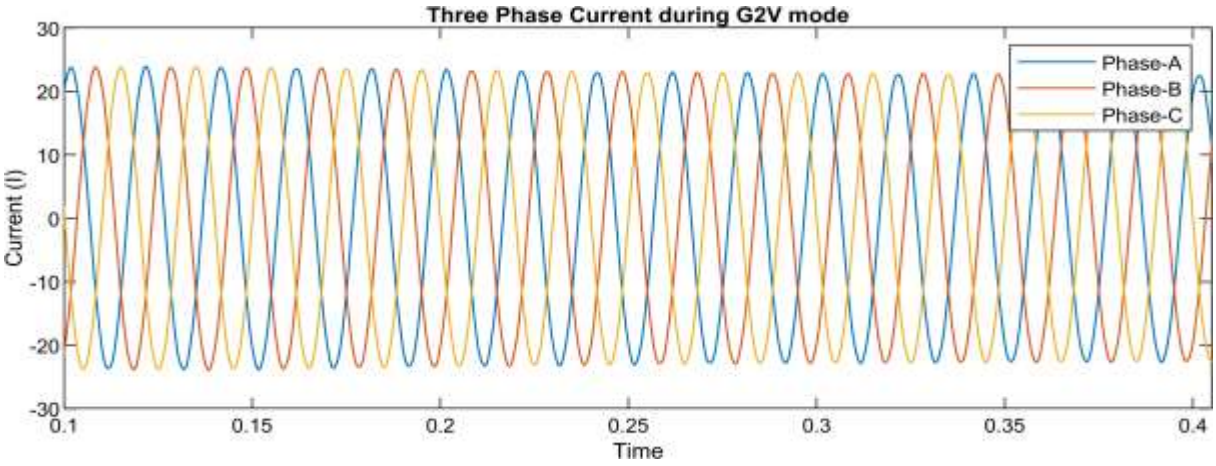

Figure 26: *In the figure, the graphs of all the three phases of currents are displayed during the charging mode.*

In FIGURE 27, DC voltage before the buck converter and after the rectification is displayed.

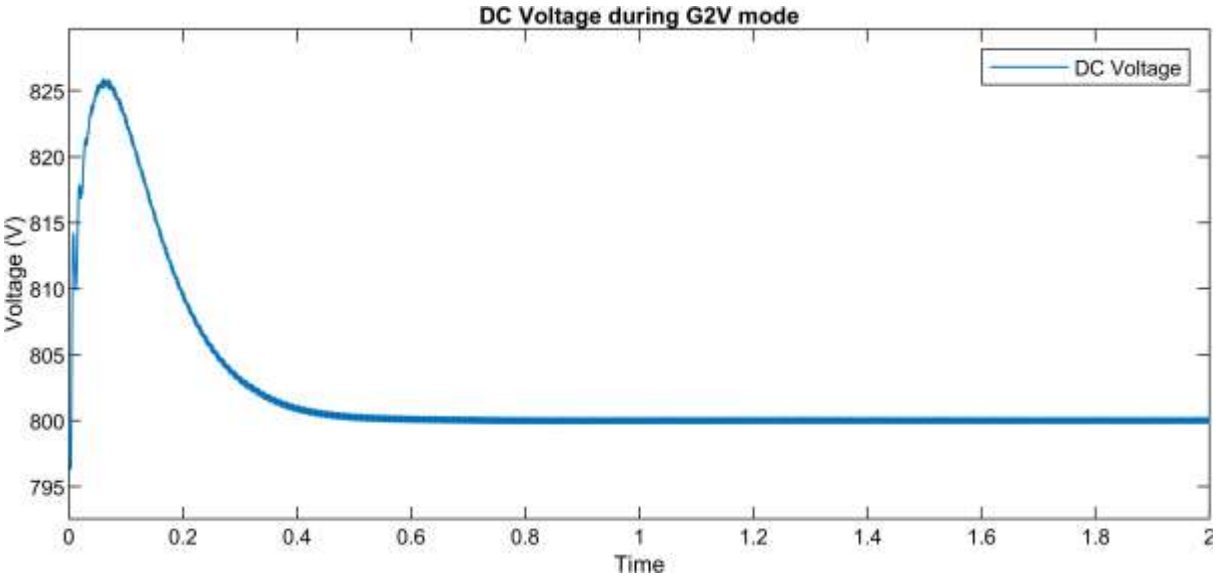

Figure 27: *This displays the graph of DC voltage before buck converter during charging mode.*

The battery voltage during the charging mode is shown in **FIGURE 28.**

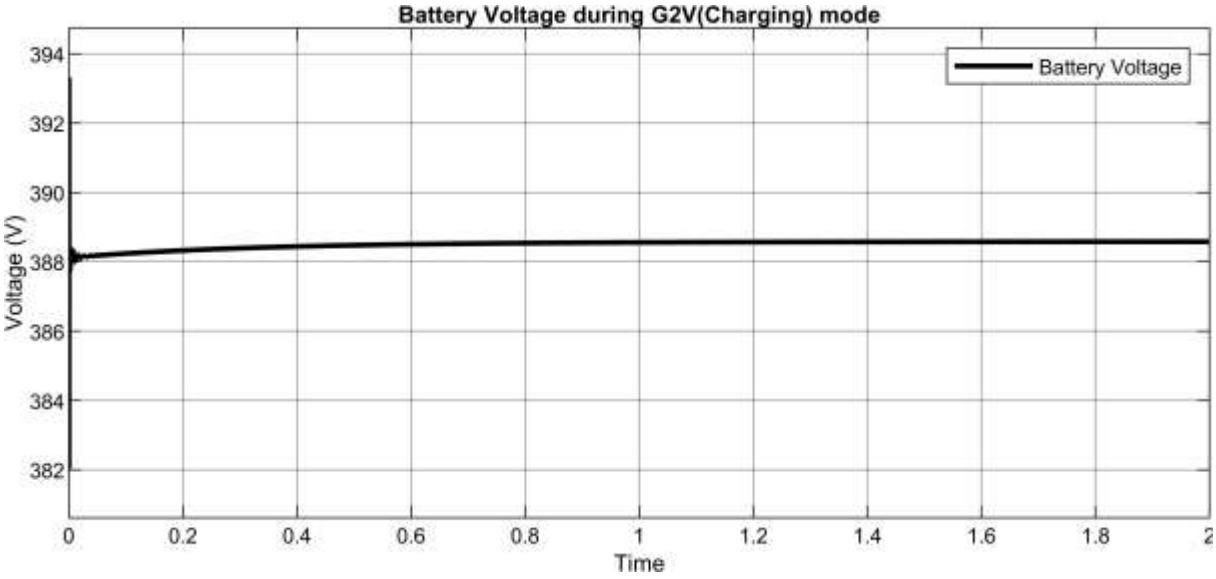

Figure 28: *DC Battery voltage during charging mode.*

The battery current during the charging mode is shown in **FIGURE 29.**

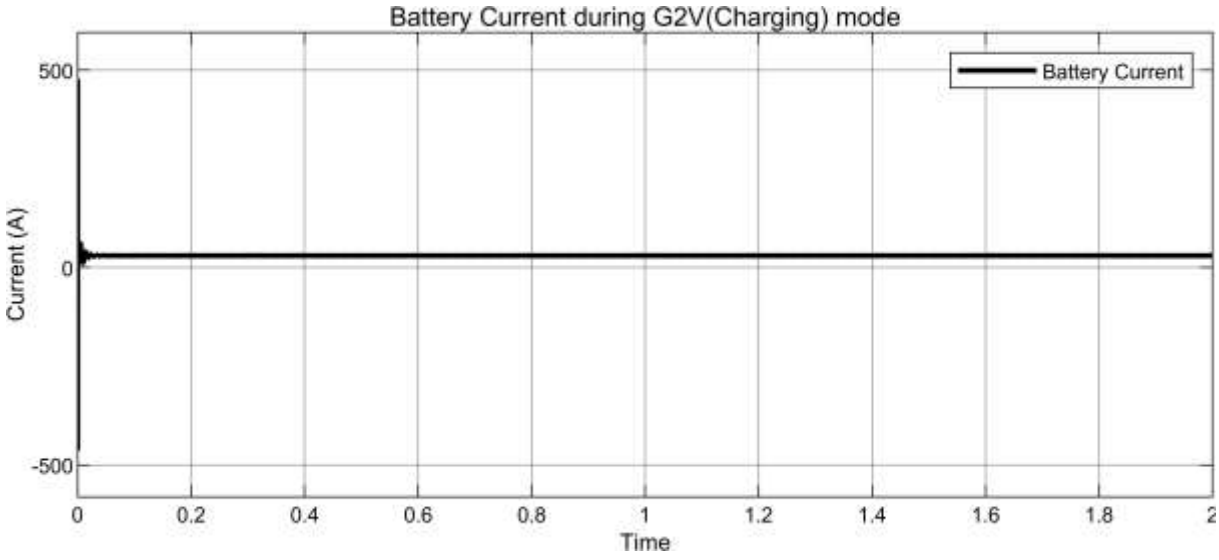

Figure 29: *Battery Current during charging mode.*

The real power consumed by the bidirectional charger during the charging mode is shown in **FIGURE 30**.

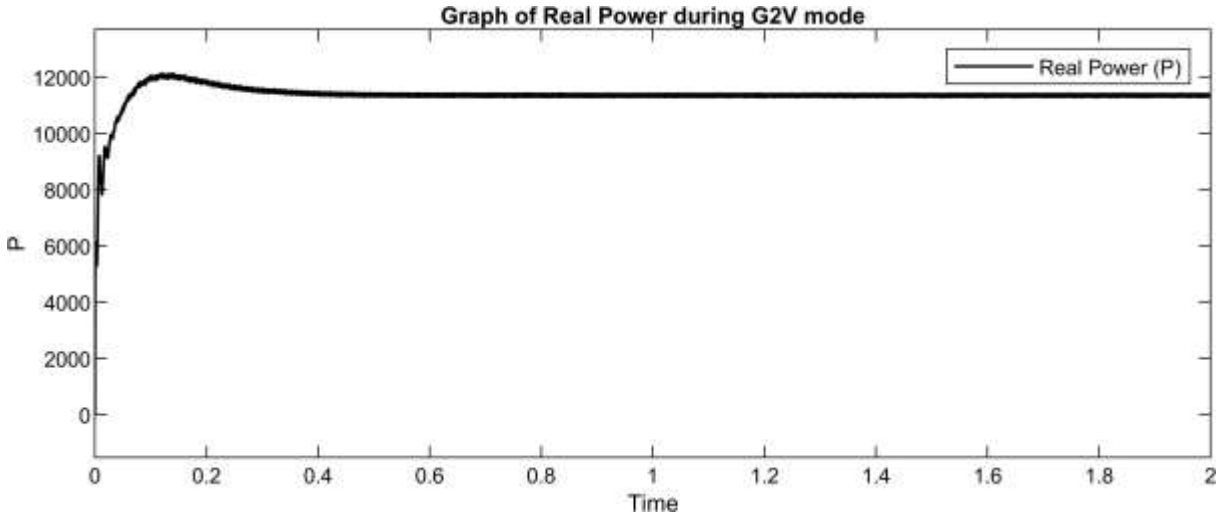

Figure 30: *Consumption of real power by the bidirectional charger is shown in this figure.*

The reactive power consumed by the bidirectional charger during the charging mode is shown in FIGURE 31.

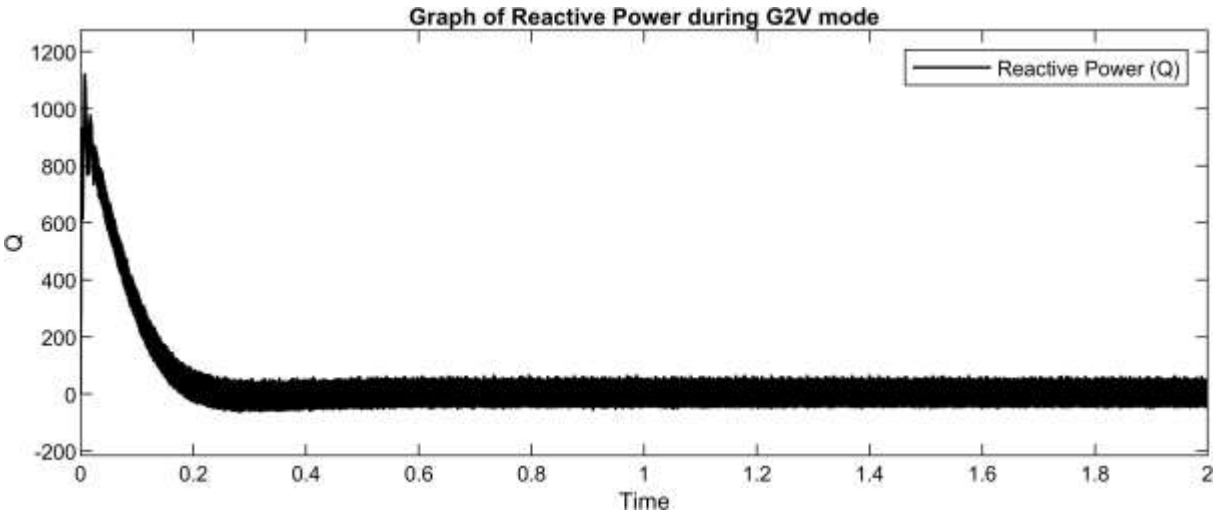

Figure 31: *Consumption of reactive power by the bidirectional charger is shown in this figure.*

The three-phase voltage from the main bus of all the synchronized generation units i.e., Utility grid, Diesel generator, Wind generator, and PV generator in V2G mode are displayed in FIGURE 32. The results display that all the phases of voltages are balanced 120 degrees apart.

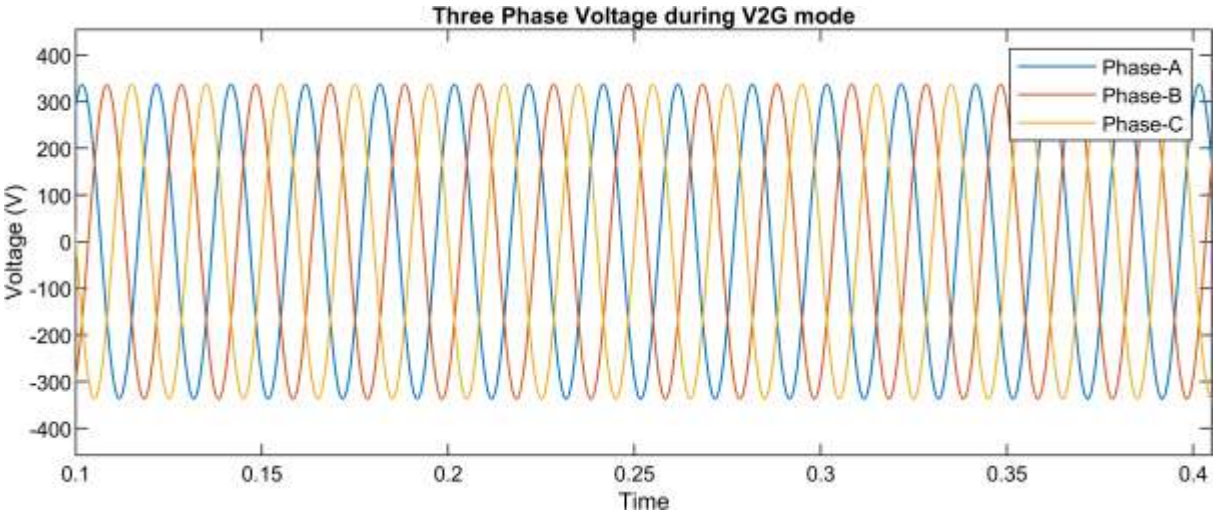

Figure 32: *In the above figure the graphs of three-phase voltages are shown for the discharging mode.*

The three-phase current from the main bus of all the synchronized generation units i.e., Utility grid, Diesel generator, Wind generator, and PV generator are displayed in FIGURE 33. It indicates that all the phases are balanced, currents are in-phase and exactly 120 degrees apart.

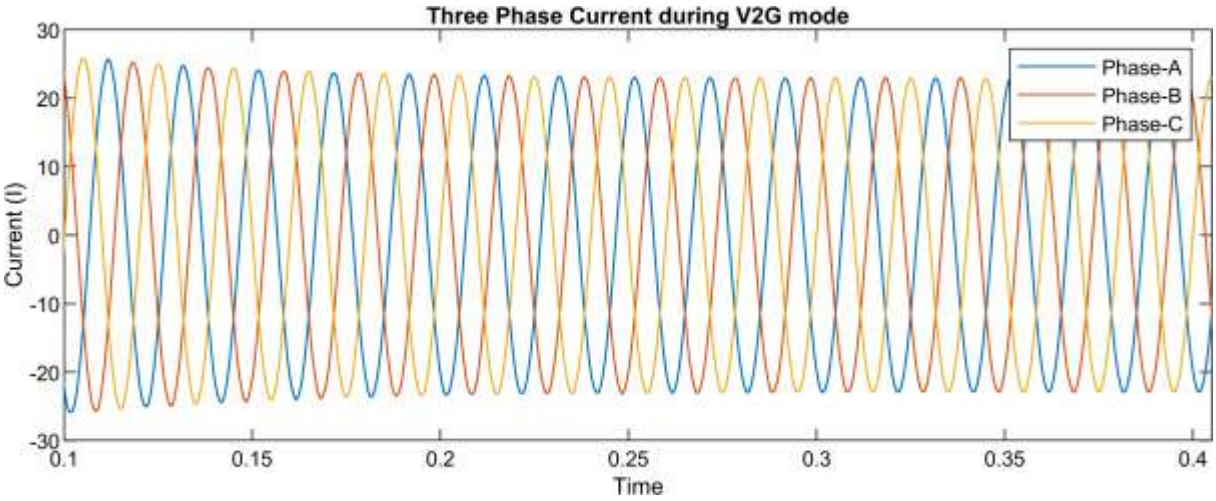

Figure 33: *In the above figure the graphs of three-phase voltages are shown for the charging mode.*

DC voltage of the batteries of EV after the boost converter and before the three-phase inverter during dis-charging mode is shown in FIGURE 34.

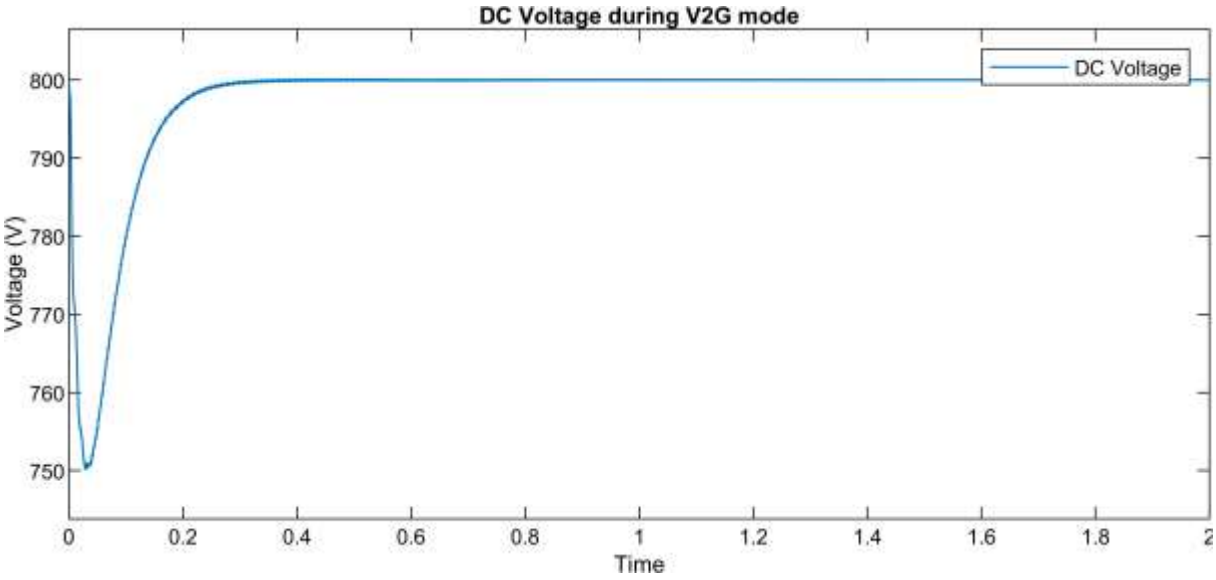

Figure 34: *DC Voltage of the battery after the boost converter and before the main three-phase inverter is displayed in this figure.*

The battery voltage during the discharging mode is shown in **FIGURE 35.**

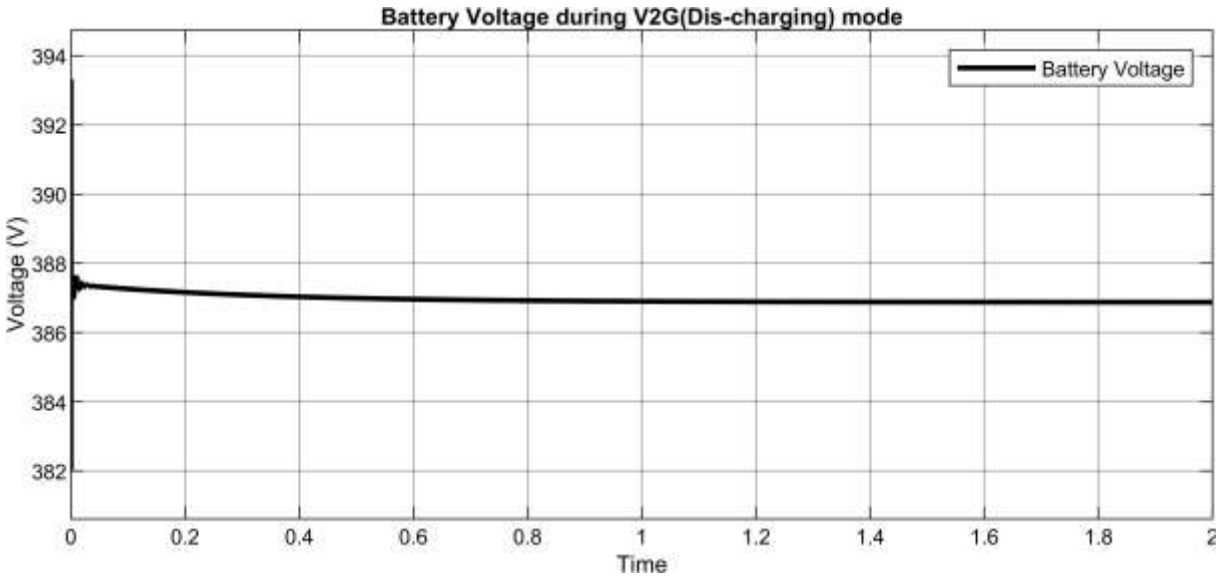

Figure 35: *DC Battery voltage during the V2G mode.*

The battery current during the discharging mode is shown in **FIGURE 36.**

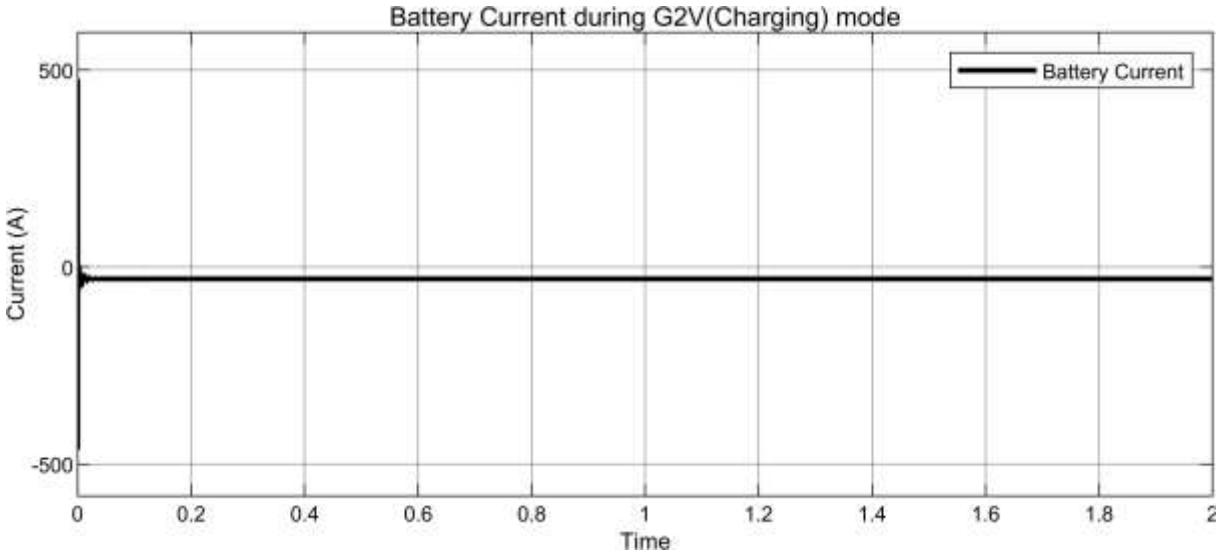

Figure 36: *Battery current during the V2G mode.*

Real power provided by the bidirectional charger during the V2G mode is shown in this FIGURE 37.

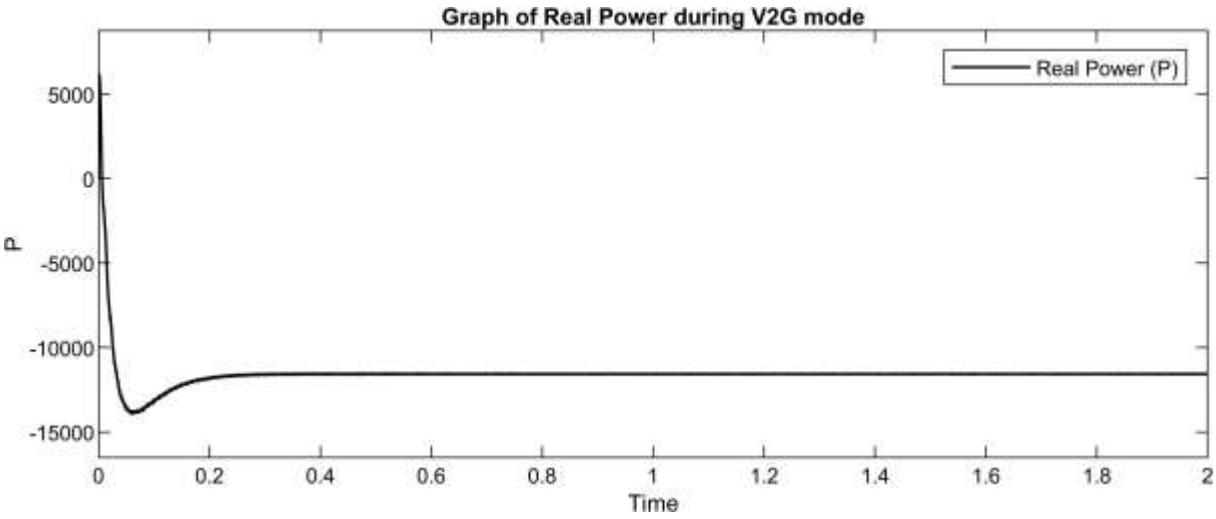

Figure 37: *Real power provided by the bidirectional charger during the V2G mode is shown in this figure.*

Reactive power provided by the bidirectional charger during the V2G mode is shown in FIGURE 38.

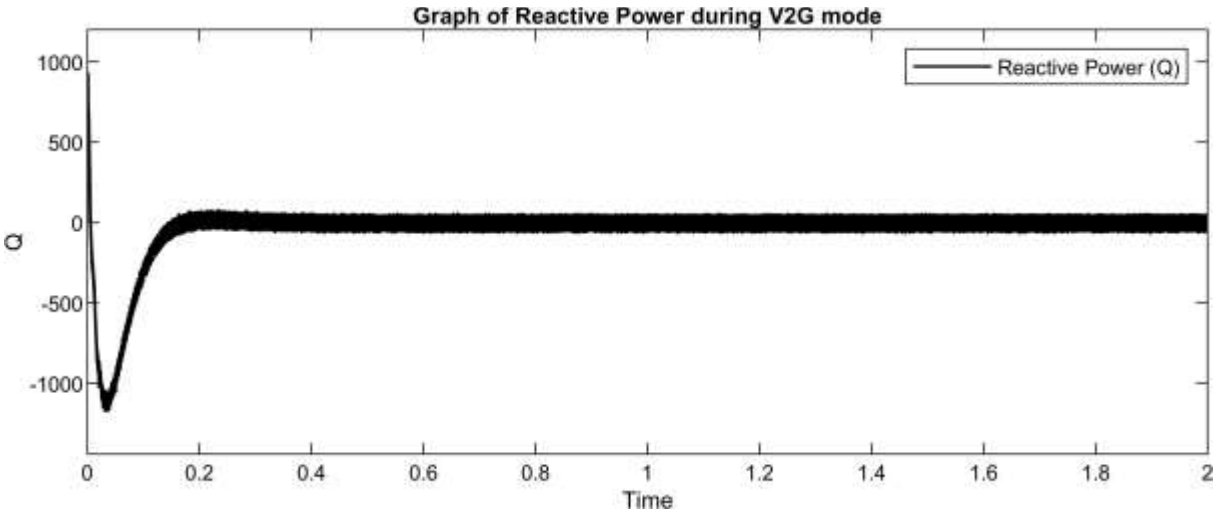

Figure 38: *Reactive power provided by the bidirectional charger during the V2G mode is shown in this figure.*

5 Results Comparison and Discussion

The microgrid is designed in the first step in which multiple generators are designed i.e., photovoltaic generator, wind generator and diesel generator. By keeping the same frequency, voltage, and phase sequence all the three are synchronized to manage optimal loading. Then through a step-down transformer, the voltage is stepped down for the secondary distribution level. In the results and the simulations section, the voltage and current waveforms are displayed. Batteries of EVs are also connected at the secondary distribution level for V2G mode or G2V mode. In G2V mode DC voltage after the three-phase converter is also shown the same graphically. The positive real power in **FIGURE 30** indicates that the real current is in the forward direction and the EV is consuming the power from the grid. The graph of the DC voltage of the battery shown in **FIGURE 28** indicates that the voltage of the battery is rising slowly with the charging of the battery.

5.1 Comparison:

A comparison between DC charging voltage , DC discharging voltage , discharging real and reactive power of the [30] to our system results are shown in the following sections.

5.1.1 Comparison between DC charging voltages:

. It can be seen from the below **FIGURE 39** that due to switching devices and charging devices, reaching the steady stage of DC charging voltage is taking more than one second. However, in our proposed scheme from **FIGURE 40**, it can be seen that the steady-state is achieved in less than 0.1s.

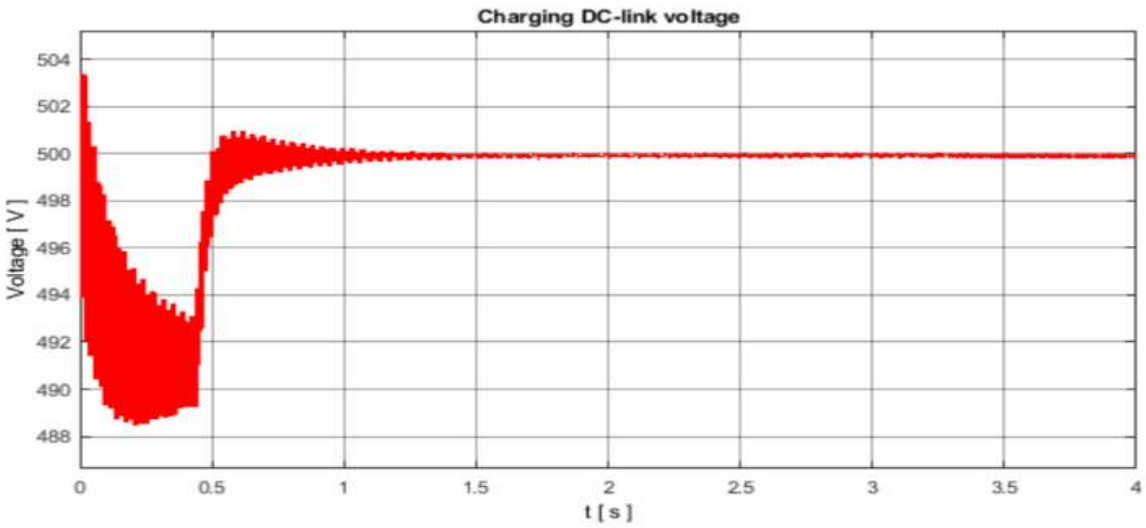

Figure 39: *The graph of DC charging voltage in G2V mode from [30].*

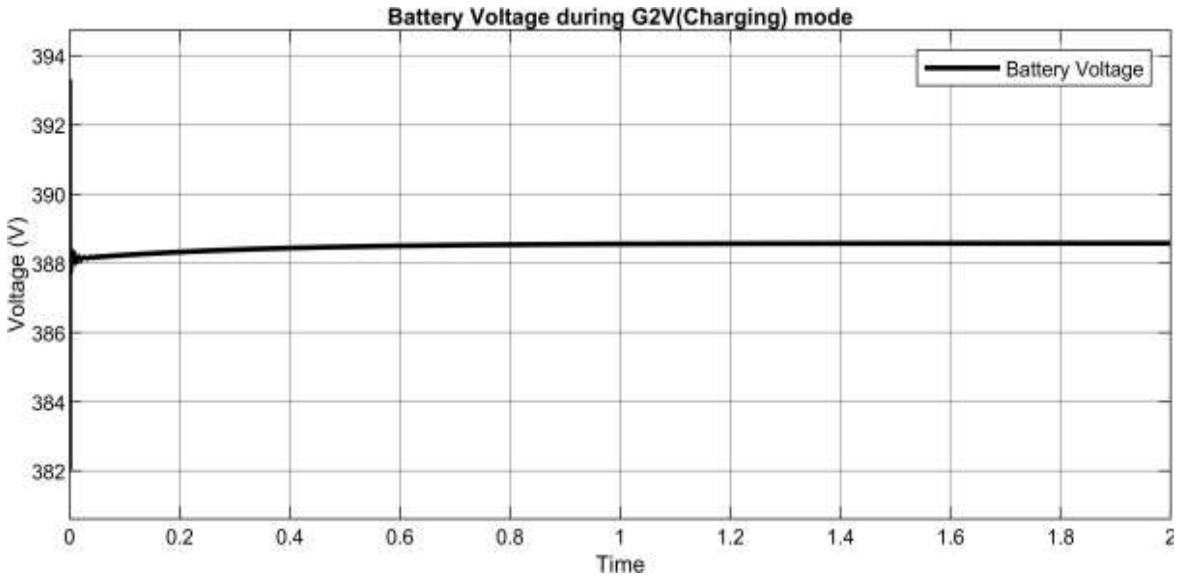

Figure 40: *DC Battery voltage during charging mode.*

5.1.2 Comparison Between Reactive Power:

In **FIGURE 41** reactive power is zero throughout so it cannot be used as a static VAR compensator but our proposed bidirectional charger EV can be used as a static VAR compensator as it can be seen from **FIGURE 42.**

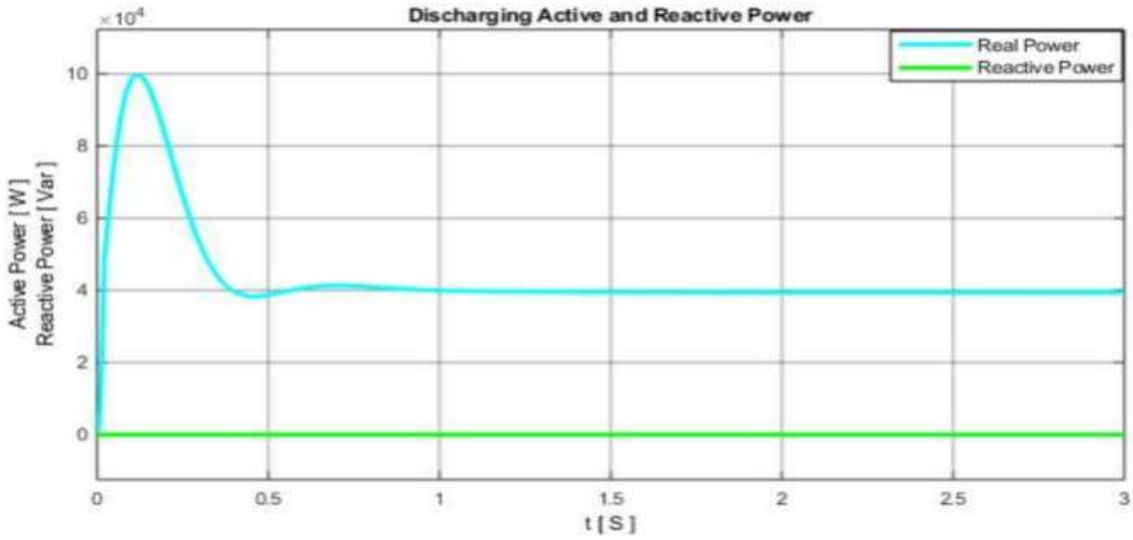

Figure 41: *The graph of discharging real and reactive power in G2V mode [30].*

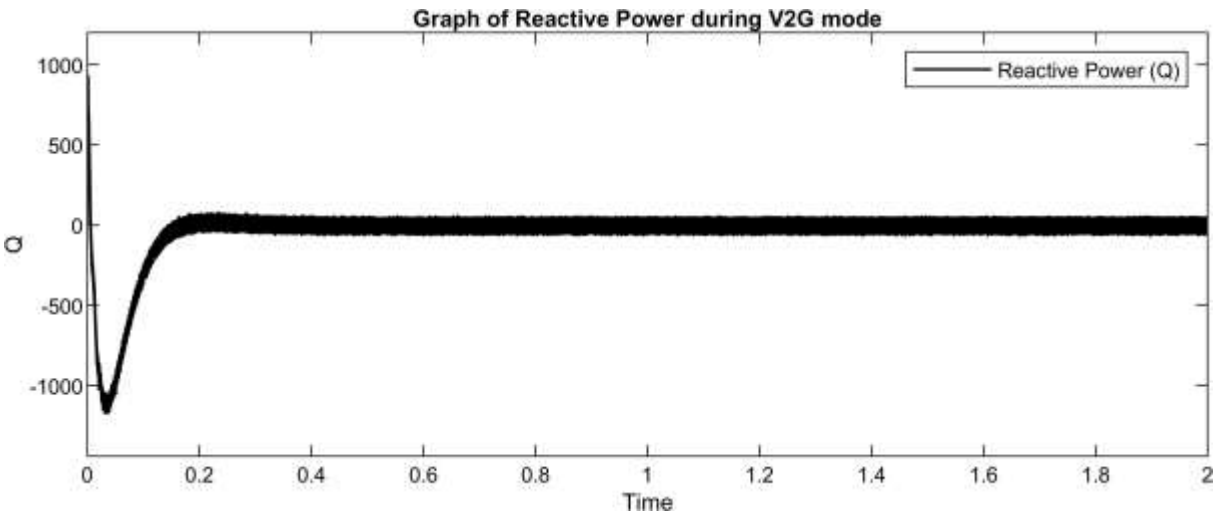

Figure 42: *Reactive power provided by the bidirectional charger during the V2G mode is shown in this figure.*

For V2G mode graphs of three-phase AC voltage, three-phase AC current, DC voltage before the three-phase converter and after the buck converter, real power, and reactive power is displayed in the above section. The battery DC voltage in V2G mode shown in **FIGURE 35** indicates that the voltage of the battery is decreasing slightly with the time as the battery is getting discharged.

5.1.3 Comparison Between Discharging Voltages:

It can be seen from the below **FIGURE 43** graph that due to switching devices and charging devices, to reach the steady stage discharging voltage is taking more than one second. However, in our proposed scheme from **FIGURE 44**, it can be seen that the steady-state is achieved in less than 0.1second.

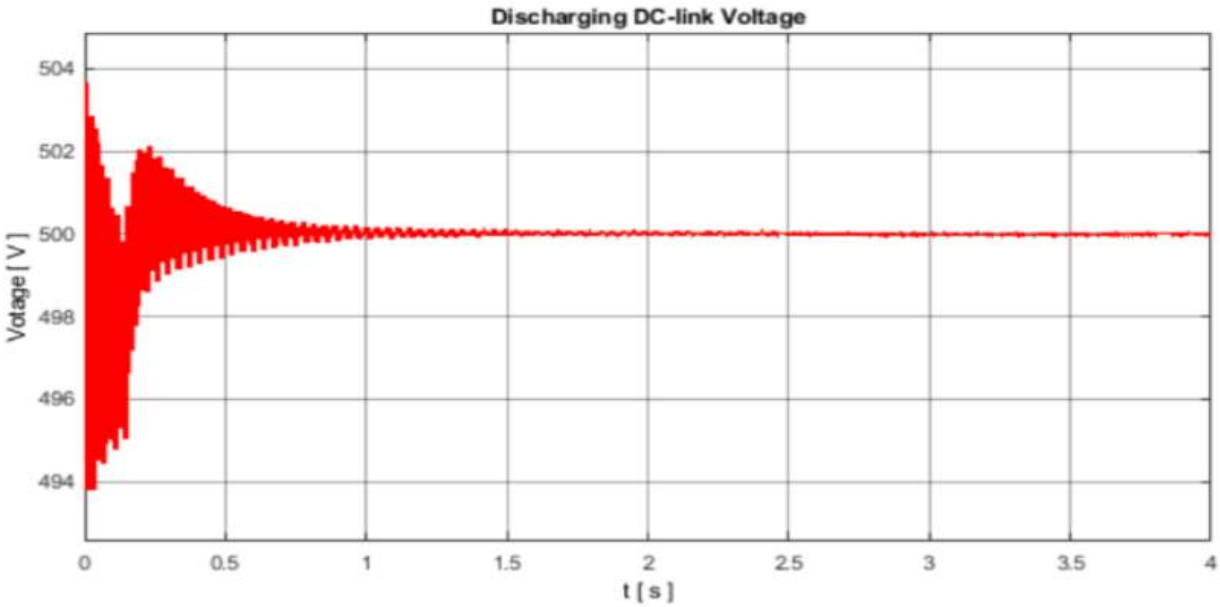

Figure 43: *The graph of DC dis-charging voltage in V2G mode [30]*

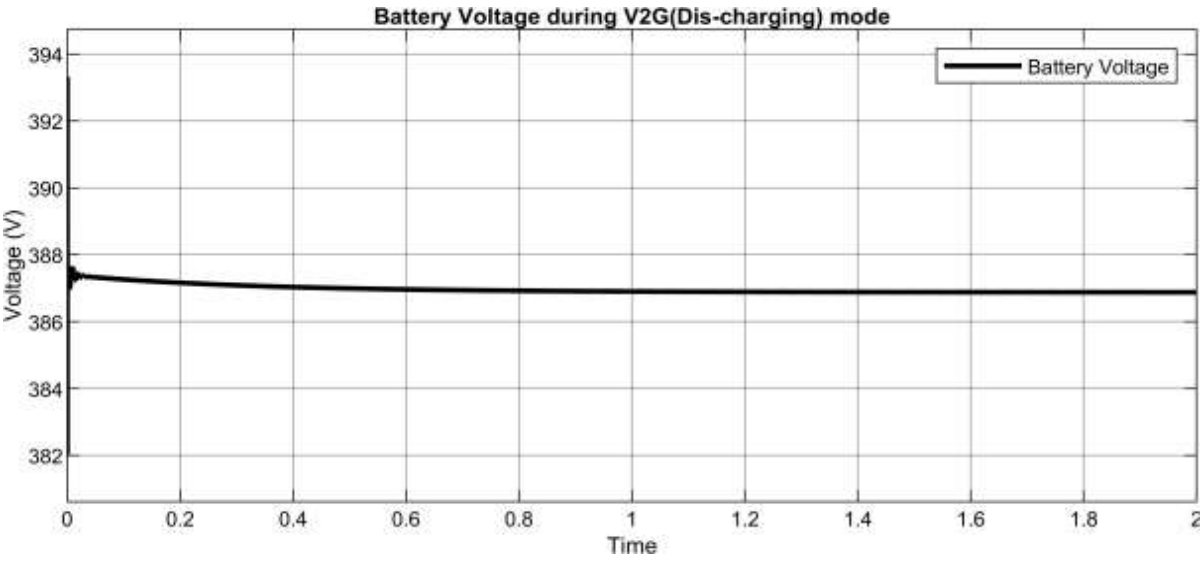

Figure 44: *DC Battery voltage during the discharging V2G mode.*

The negatively valued graph of real power indicates that current is flowing in the reverse direction and power is EV is supplying power to the grid. All the results have been shown quantitatively, proving that our bidirectional charger has the ability to perform in both V2G and G2V mode efficiently. Therefore, our proposed technique is far better than the state-of-the-art techniques in terms of performance and power quality concerns as batteries of EVs are one of the most expensive components and by improving the power quality we can increase their life.

A highlight of our comparison of results is shown in the following TABLE 4:

Table 4: *Table of Contributions and Comparison with the state-of-the-art technique*

Variable	[30]	Our System
Flow of Forward Real Power	Yes	Yes
Flow of Reverse Real Power	Yes	Yes
Flow of Forward Reactive Power	No	Yes
Flow of Reverse Reactive Power	No	Yes
Time to reach Steady State	*1.2s*	0.02s
Transients	*-2.5% - +1%*	*-0.1% - +0.05%*

6 Conclusion

A three-phase, two stages off-board bidirectional EV charger is proposed. The first stage rectifies the three-phase grid voltage for charging purposes while the later stage attenuates the rectified DC bus voltage to a magnitude level suitable for battery charging and vice versa. The power factor correction enables the exchange of both active and reactive powers between the two entities. The grid side LCL filter works perfectly to keep the total harmonic distortion of grid current within the encapsulated range of approximately 5%. The DC link voltage remains constant for all operational scenarios and there is no spike or overshoot while switching between modes or even if the grid side voltage is disturbed somehow. The detailed analytical assessment of the results for both charging and discharging modes verifies the robustness of the proposed design and control and proves the feasibility of its practical implementation.

Works Cited

[1] V. G. Saber AY, «One million plug-in electric vehicles on the road by 2015,» *Proceedings of IEEE Intell Transaction Systems,* p. 141– 147, Oct 2009.

[2] L. a. L. H. Hockstad, «Inventory of US greenhouse gas emissions and sinks,» 2018.

[3] C. C. Chan, «The State of the Art of Electric, Hybrid, and Fuel Cell Vehicles,» *Proceedings of the IEEE,* vol. 95, pp. 704-718, 2007.

[4] S. B. C. A. A.-H. K. P. A. K. D. Singh B, «A review of three-phase improved power quality AC–DC converters,» *IEEE Transaction Ind Electronics,* pp. 641- 660, 2004.

[5] B. J., «Automotive Electricity,» i *Wiley,* New York, 2010..

[6] G.-K. P. R. K. a. P. F. S. Solomon, «Irreversible climate change due to carbon dioxide emissions,» *Proceedings of the National Academy of Sciences,* vol. 106, pp. 1704-1709, Feb. 2009.

[7] A. M. T. T. Grenier M, «Design of on-board charger for plug-in hybrid electric vehicle,» *Proc Power Electronics Machine and Drives,* vol. 6, p. 1–6, 2010.

[8] K. K. L. S. e. a. Haghbin S, «Integrated chargers for EV's and PHEV's: Examples and new solutions,» *Proc. Int. Conf. Electrical Machines,* p. 1– 6, 2010.

[9] L. C. Chang HC, «Development of a compact switched-reluctance motor drive for EV propulsion with voltage-boosting and PFC charging capabilities,» *IEEE Trans. Veh. Technol,* vol. 58, pp. 3198- 3215, 2009.

[10] R. WE., «Integrated traction inverter and battery charger apparatus,» *U.S. Patent,* Apr. 1990.

[11] «Communication Networks and Systems in Substations—Basic Communication Structure—Distributed Energy Resources Logical Nodes,» vol. Edition 1.0, 2009.

[12] T. S. U. e. al., «Distributed energy resources (DER) object modeling with IEC 61850-7-420,» 2011.

[13] T. S. U. e. al., «Extending IEC 61850-7-420 for distributed generators with fault current limiters,» 2011.

[14] «Communication Networks and Systems for Power Utility Automation--IEC 61850 Object Models for Electric Mobility,» 2012.

[15] W. W. K. a. S. H. Schneider, «Global Air Pollution and Climate Change,» *IEEE Transactions on Geoscience Electronics,* vol. 16, pp. 44-50, 1978.

[16] R. R. e. a. M. S. J. Hansen, «Dangerous human-made interference with climate: a GISS modelE study,» *Atmos. Chem. Phys*, pp. 2287-2312, 2007.

[17] T. S. B. a. M. R. Sindhu, «Design and Power Management of Solar Powered Electric Vehicle Charging Station with Energy Storage System,» i *3rd International conference on Electronics, Communication and Aerospace Technology (ICECA)*, Jun. 2019.

[18] R. D. a. S. P. Karthikeyan, «An Efficient EV Fleet Management For Charging At Workplace Using Solar Energy,» i *National Power Engineering Conference (NPEC)*, Mar. 2018.

[19] C. Lampton, «How Electric Car Batteries Work,» Aug. 18, 2008. [Internett]. Available: http://auto.howstuffworks.com/fuel-efficiency/vehicles/electric-carbattery3.htm.

[20] «http://www.febeliec.be/,» 2022. [Internett].

[21] J. H. A. S. M. E.-C. L. F. &. U. S. Yusuf, «A Centralized Optimization Approach for Bidirectional PEV Impacts Analysis in a Commercial Building-Integrated Microgrid,» 2021.

[22] S. A. N. B. A. P. B. C. B. &. T. C. Hashemi, «Frequency regulation provision using cross-brand bidirectional V2G-enabled electric vehicles,» August, 2018.

[23] J. T. H. H. W. Y. H. T. &. L. D. Liao, «Decentralized V2G/G2V scheduling of EV charging stations by considering the conversion efficiency of bidirectional chargers,» 2021.

[24] D. X. G. &. X. Y. Sha, «Utility direct interfaced charger/discharger employing unified voltage balance control for cascaded H-bridge units and decentralized control for CF-DAB modules,» 2017.

[25] D. Erb, O. Onar og A. Khaligh, «Bi-directional charging topologies for plugin hybrid electric vehicles,» i *Applied Power Electronics Conference and Exposition (APEC)*, Feb. 2010.

[26] J. Gallardo-Lozano, M. Milanes-Montero, M. Guerrero-Martinez og E. RomeroCadaval, «Three-phase bidirectional battery charger for smart electric vehicles,» i *Compatibility and Power Electronics (CPE)*, June 2011.

[27] N. Weise, K. Mohapatra og N. Mohan, «Universal utility interface for Plugin Hybrid electric vehicles with vehicle-to-grid functionality,» i *Power and Energy Society General Meeting*, July 2010.

[28] S. Vaishnav og H. Krishnaswami, «Single-stage isolated bi-directional converter topology using high frequency AC link for charging and V2G applications of PHEV,» i *Vehicle Power and Propulsion Conference (VPPC)*, Sept. 2.

[29] D. M. D. a. M. H. K. R. W. A. De Doncker, «A three-phase soft switched high-power-density DC/DC converter for high-power applications,» *IEEE Transactions on Industry Applications*, 1991.

[30] O. K. Habte, «Masters Thesis: Bidirectional Power Transfer between Grid and Electric Vehicle Batteries,» University of South-Eastern, Norway, 2020.

[31] N. &. K. M. Wong, «A review of bidirectional on-board charger topologies for plugin vehicles,» i *25th IEEE Canadian Conference on Electrical and Computer Engineering (CCECE)*, Canada, 2012.

[32] M. K. M. C. &. T. L. M. Kesler, «Vehicle-to-grid reactive power operation using plug-in electric vehicle bidirectional offboard charger,» *IEEE Transactions on Industrial Electronics*, pp. 6778-6784, 2014.

[33] J. Y. R. V. K. T. K. M. a. M. N. Yong, «A review on the state-of-the-art technologies of electric vehicle, its impacts and prospects,» *Renewable and Sustainable Energy Reviews*, p. 49:365–385, 2015.

[34] D. M. F. &. B. R. Cittanti, «Optimal design of grid-side LCL filters for electric vehicle ultra-fast battery chargers,» September, 2020.

[35] Y. J. &. K. H. Kim, «Optimal design of LCL filter in grid-connected inverters,» 2019.

[36] C. P. M. C. F. M. R. &. M. A. Mahamat, «Optimized design of an LCL filter for grid connected photovoltaic system and analysis of the impact of neighbors' consumption on the system,» 2017.

[37] ed., «"The Electricity Safety, Quality and Continuity Regulations,» 2002.

[38] S. K. A. S. I. A. &. A. H. J. Albatran, «Optimal design of passive RC-damped LCL filter for grid-connected voltage source inverters,» 2018.

[39] X. W. X. P. D. Y. D. L. W. &. B. C. Ruan, «Control techniques for LCL-type grid-connected inverters,» i *Springer*, Singapore, 2018.

[40] F. J. F. G. H. L. H. &. W. Z. Li, «Research on integrated bidirectional control of EV charging station for V2G,» i *2nd International Conference on Power and Renewable Energy (ICPRE)*, 2017.

[41] F. Richter, «Statista,» [Internett]. Available: https://www.statista.com/chart/21083/tesla-cumulative-vehicle-production/.